




On the approximation of derivative values using a WENO algorithm with progressive order of accuracy close to discontinuities

Sergio Amat¹ · Juan Ruiz-Álvarez¹ · Chi-Wang Shu² · Dionisio F. Yáñez³ 

Received: 25 November 2021 / Revised: 18 April 2022 / Accepted: 15 August 2022 /

Published online: 1 September 2022

© The Author(s) 2022

Abstract

In this article, we introduce a new WENO algorithm that aims to calculate an approximation to derivative values of a function in a non-regular grid. We adapt the ideas presented in [Amat et al., SIAM J. Numer. Anal. (2020)] to design the nonlinear weights in a manner such that the order of accuracy is maximum in the intervals close to the discontinuities. Some proofs, remarks on the choice of the stencils and explicit formulas for the weights and smoothness indicators are given. We also present some numerical experiments to confirm the theoretical results.

Keywords WENO-2r · High accuracy interpolation · Improved adaption to discontinuities · Generalization

Mathematics Subject Classification 65D25 · 65D15 · 68W25

1 Introduction and review: central WENO and motivation

In this paper, we design a family of central weighted essentially non-oscillatory (CWENO) schemes that allows to approximate derivative values. We are inspired by the algorithm

Communicated by Jose Alberto Cuminato.

The work of the first and second authors was supported by project 20928/PI/18 (Proyecto financiado por la Comunidad Autónoma de la Región de Murcia a través de la convocatoria de Ayudas a proyectos para el desarrollo de investigación científica y técnica por grupos competitivos, incluida en el Programa Regional de Fomento de la Investigación Científica y Técnica (Plan de Actuación 2018) de la Fundación Séneca-Agencia de Ciencia y Tecnología de la Región de Murcia), by the national research project PID2019-108336GB-I00 (MINECO/FEDER). The work of the third author was supported by NSF Grant DMS-2010107 and AFOSR Grant FA9550-20-1-0055. The work of the fourth author was supported by grant PID2020-117211GB-I00 funded by MCIN/AEI/10.13039/501100011033.

✉ Dionisio F. Yáñez
dionisio.yanez@uv.es

Extended author information available on the last page of the article

employed by Levy et al. in Levy et al. (1999), which is designed to approximate solutions of hyperbolic systems of conservation laws,

$$\begin{cases} u_t + f(u)_x = 0, & u \in \mathbb{R}^2, \\ u(x, 0) = u_0(x). \end{cases}$$

In our case, the motivation would be the possible application of the new algorithm to obtain approximations of the solution of Hamilton–Jacobi type equations,

$$\begin{cases} \varphi_t + H(\varphi_x) = 0, \\ \varphi(x, 0) = \varphi_0(x), \end{cases} \tag{1}$$

where algorithms that use interpolation to get accurate approximations to the derivative φ_x have been proved to be very useful. In what follows, we show the construction of the algorithm and provide theoretical and numerical proofs of its accuracy, but we let the solution of the equation in (1) to be future work. Even so, as we show in what follows, the algorithm proposed can be used as a general technique to obtain the derivatives of a function with singularities, providing progressive order of accuracy close to these singularities.

In Levy et al. (1999), the authors use a uniform discretization in time but not in space, i.e. $x_i = h_i$ are the spatial grid points and $t^n = n\Delta t$ are the time steps. In Levy et al. (1999), two reconstructions are necessary to design the method: firstly, a reconstruction scheme to approximate the average of the function u over a cell at a time t^n ; secondly, a reconstruction of f for the derivative of the fluxes, Q_i , which satisfies:

$$\frac{\partial Q_i}{\partial x}(x_i, t^n) =: Q'_i(x_i, t^n) = f'(u(x_i, t^n)) + O(h^{r-1}), \tag{2}$$

where $r - 1$ is the accuracy attained for the reconstruction of the derivative, and supposing that u at a time t^n is known. WENO nonlinear interpolation methods can be used for this purpose (see e.g. Levy et al. (1999); Liu et al. (1994); Shu (1999)). In Levy et al. (1999), a symmetric strategy is used, but in this work, we construct a general method that is not necessarily symmetric. Therefore, in this paper, we will construct a new nonlinear method to approximate the derivative point values with progressive order of accuracy close to the discontinuities adapting the ideas presented in Amat et al. (2020). We will present this method for any r . We reformulate this problem as follows:

We suppose $[a, b] \subset \mathbb{R}$ and a grid $X = \{x_j\}_{j=0}^J$, $x_0 = a$, $x_J = b$, $x_{j+1} = x_j + h_j$, $x_{j+1/2} = x_j + h_j/2$, $x_{j-1/2} = x_j - h_{j-1}/2$, $h = \max\{h_j : j = 0, \dots, J - 1\}$, and we suppose that there exists $L > 0$ such that

$$\tilde{h} = \frac{\max\{h_j : j = 0, \dots, J - 1\}}{\min\{h_j : j = 0, \dots, J - 1\}} = \frac{h}{\min\{h_j : j = 0, \dots, J - 1\}} \leq L.$$

For a piecewise smooth function f , we consider a point value discretization $f(x_j) = f_j$, $j = 0, \dots, J$. To calculate the derivative value at a specific point x_i , we take the stencils of r points which contain it, i.e. let $\mathcal{I}_{i,k}^r = \{i - (r - 1) + k, \dots, i + k\}$ be the subindex and the stencils $\mathcal{S}_{i,k}^r = \{x_t : t \in \mathcal{I}_k^i\}$ with $k = 0, \dots, r - 1$ and calculate the interpolation polynomial of degree $r - 1$ such that $p_{i,k}^{r-1}(x_j) = f_j$, $j \in \mathcal{I}_{i,k}^r$. The classic WENO interpolator is a convex combination of these polynomials:

$$P_i(x) = \sum_{k=0}^{r-1} \omega_{i,k}^{r-1} p_{i,k}^{r-1}(x),$$

where $\omega_{i,k}^{r-1}$ are nonlinear weights whose value depends on the existence of a discontinuity affecting the stencil. In our case, we will define

$$(P_i)'(x_i) = \frac{dP_i}{dx}(x_i) = \sum_{k=0}^{r-1} \omega_{i,k}^{r-1} \frac{dp_{i,k}^{r-1}}{dx}(x_i). \tag{3}$$

It is clear that if the function is smooth at the largest stencil $\{x_{i-(r-1)}, \dots, x_{i+(r-1)}\}$, then, if the choice of the nonlinear weights is adequate, we can obtain an approximation of the derivative values of order of accuracy $O(h^{2r-2})$. However, when a discontinuity crosses the above-mentioned stencil, typically (see, e.g. Liu et al. (1994)), the order decreases to $r - 1$. Note that there are two principal differences between classical WENO interpolation for point-value approximation of a function and the WENO algorithm used to obtain an approximation of the derivative values:

1. When we use classical WENO algorithm for point-value interpolation, we take the stencils which contain x_{i-1} and x_i because, typically, we interpolate at $x_{i-\frac{1}{2}}$.
2. The evaluation of the derivative of the polynomial, P_i' , Eq. (3), is at x_i not at $x_{i-\frac{1}{2}}$.

The key of this method is the definition of the nonlinear weights that make use of linear optimal weights and that are defined as follows. Let $p_{i,0}^{2r-2}$ be the polynomial which interpolates f at $\{x_{i-(r-1)}, \dots, x_{i+(r-1)}\}$, then there exist $C_{i,k}^{r-1} > 0, k = 0, \dots, r - 1$ which satisfy:

$$\frac{dp_{i,0}^{2r-2}}{dx}(x_i) = \sum_{k=0}^{r-1} C_{i,k}^{r-1} \frac{dp_{i,k}^{r-1}}{dx}(x_i), \quad \sum_{k=0}^{r-1} C_{i,k}^{r-1} = 1. \tag{4}$$

The following proposition for non-uniform grid is proved in Yáñez (2010) using the ideas proposed in Arándiga et al. (2010). We reproduce it here for completeness.

Proposition 1.1 *The optimal weights are determined by:*

$$C_{i,0}^{r-1} = \prod_{s=i+1}^{i+(r-1)} \frac{x_i - x_s}{x_{i-(r-1)} - x_s},$$

$$C_{i,k}^{r-1} = \prod_{s \in \mathcal{I}_{i,0}^{2r-1} \setminus \mathcal{I}_{i,k}^r} \frac{x_i - x_s}{x_{i-(r-1)+k} - x_s} - \sum_{t=0}^{k-1} C_{i,t}^{r-1} \prod_{s \in \mathcal{I}_{i,t}^r \setminus \mathcal{I}_{i,k}^r} \frac{x_i - x_s}{x_{i-(r-1)+k} - x_s} \tag{5}$$

$$\prod_{s \in \mathcal{I}_{i,k}^r \setminus \mathcal{I}_{i,t}^r} \frac{x_{i-(r-1)+k} - x_s}{x_i - x_s},$$

with $0 \leq k < r - 1$.

Proof Using Lagrange’s base, we know that:

$$L_{j,k}^{r-1}(x) = \prod_{\substack{t=i-(r-1)+k \\ t \neq j}}^{i+k} \frac{x - x_t}{x_j - x_t},$$

then:

$$p_{i,k}^{r-1}(x) = \sum_{j=i-(r-1)+k}^{i+k} f_j L_{j,k}^{r-1}(x) \Rightarrow \frac{d}{dx} p_{i,k}^{r-1}(x) = \sum_{j=i-(r-1)+k}^{i+k} f_j \frac{d}{dx} L_{j,k}^{r-1}(x),$$

with

$$\frac{d}{dx} L_{j,k}^{r-1}(x) = \sum_{s=i-(r-1)+k}^{i+k} \frac{1}{x_j - x_s} \prod_{\substack{t=i-(r-1)+k \\ t \neq j,s}}^{i+k} \frac{x - x_t}{x_j - x_t}.$$

Therefore:

$$\begin{aligned} \frac{d}{dx} p_{i,k}^{r-1}(x_i) &= \sum_{\substack{j=i-(r-1)+k \\ j \neq i}}^{i+k} \left(\frac{f_i}{x_i - x_j} + \frac{f_j}{x_j - x_i} \prod_{\substack{s=i-(r-1)+k \\ s \neq i,j}}^{i+k} \frac{x_i - x_s}{x_j - x_s} \right) \\ &= \sum_{j \in \mathcal{I}_{i,k}^r \setminus \{i\}} \left(\frac{f_i}{x_i - x_j} + \frac{f_j}{x_j - x_i} \prod_{s \in \mathcal{I}_{i,k}^r \setminus \{i,j\}} \frac{x_i - x_s}{x_j - x_s} \right). \end{aligned}$$

Analogously:

$$\frac{d}{dx} p_{i,0}^{2r-2}(x_i) = \sum_{j \in \mathcal{I}_{i,0}^{2r-1} \setminus \{i\}} \left(\frac{f_i}{x_i - x_j} + \frac{f_j}{x_j - x_i} \prod_{s \in \mathcal{I}_{i,0}^{2r-1} \setminus \{i,j\}} \frac{x_i - x_s}{x_j - x_s} \right).$$

We can obtain the optimal weights from the equality:

$$\frac{d}{dx} p_{i,0}^{2r-2}(x_i) = \sum_{k=0}^{r-1} C_{i,k}^{r-1} \frac{d}{dx} p_{i,k}^{r-1}(x_i); \tag{6}$$

thus, if $k = 0$, then the unique stencil of r points which contains the point $x_{i-(r-1)}$ is $\mathcal{S}_{i,0}^r$. Then, taking the term of $f_{i-(r-1)}$, we obtain:

$$\begin{aligned} \frac{C_{i,0}^{r-1}}{x_{i-(r-1)} - x_i} \prod_{s=i-(r-1)+1}^{i-1} \frac{x_i - x_s}{x_{i-(r-1)} - x_s} &= \frac{1}{x_{i-(r-1)} - x_i} \prod_{\substack{s=i-(r-1)+1 \\ s \neq i}}^{i+(r-1)} \frac{x_i - x_s}{x_{i-(r-1)} - x_s} \rightarrow C_{i,0}^{r-1} \\ &= \prod_{s=i+1}^{i+(r-1)} \frac{x_i - x_s}{x_{i-(r-1)} - x_s}. \end{aligned}$$

Now, if we take $k = 1$, we have only two stencils: $\mathcal{S}_{i,0}^r$ and $\mathcal{S}_{i,1}^r$, which contain the point $x_{i-(r-1)+1}$. Then using Eq. (6) at term $f_{i-(r-1)+1}$, we get:

$$\begin{aligned} \frac{C_{i,0}^{r-1}}{x_{i-(r-1)+1} - x_i} \prod_{\substack{s=i-(r-1) \\ s \neq i-(r-1)+1}}^{i-1} \frac{x_i - x_s}{x_{i-(r-1)+1} - x_s} &+ \frac{C_{i,1}^{r-1}}{x_{i-(r-1)+1} - x_i} \prod_{\substack{s=i-(r-1)+2 \\ s \neq i}}^{i+1} \frac{x_i - x_s}{x_{i-(r-1)+1} - x_s} \\ &= \frac{1}{x_{i-(r-1)+1} - x_i} \prod_{\substack{s=i-(r-1) \\ s \neq i,i-(r-1)+1}}^{i+(r-1)} \frac{x_i - x_s}{x_{i-(r-1)+1} - x_s}, \\ C_{i,1}^{r-1} &= \prod_{\mathcal{I}_{i,0}^{2r-1} \setminus \mathcal{I}_{i,1}^{r-1}} \frac{x_j - x_k}{x_{j-r+1} - x_k} - C_{i,0}^{r-1} \prod_{s \in \mathcal{I}_{i,0}^r \setminus \mathcal{I}_{i,1}^r} \frac{x_i - x_s}{x_{i-(r-1)+1} - x_s} \prod_{s \in \mathcal{I}_{i,1}^r \setminus \mathcal{I}_{i,0}^r} \frac{x_{i-(r-1)+1} - x_s}{x_i - x_s}. \end{aligned}$$

We suppose that we have obtained the optimal weights $C_{i,0}^{r-1}, C_{i,1}^{r-1}, \dots, C_{i,k-1}^{r-1}$ with $0 < k < r - 1$, we will get $C_{i,k}^{r-1}$. The point $x_{i-(r-1)+k}$ is in the stencils $\mathcal{S}_{i,0}^r, \mathcal{S}_{i,1}^r, \dots, \mathcal{S}_{i,k}^r$, then

Table 1 Optimal weights for $r = 2, 3$ and a uniform grid

	$r = 2$	$r = 3$
$C_{i,0}^{r-1}$	$\frac{x_{i+1}-x_i}{x_{i+1}-x_{i-1}}$	$\frac{(x_i-x_{i+1})(x_i-x_{i+2})}{(x_{i-2}-x_{i+1})(x_{i-2}-x_{i+2})}$
$C_{i,1}^{r-1}$	$\frac{x_i-x_{i-1}}{x_{i+1}-x_{i-1}}$	$\frac{(x_i-x_{i-2})(x_i-x_{i+2})}{x_{i-2}-x_{i+2}} \left(\frac{1}{x_{i-1}-x_{i+2}} + \frac{1}{x_{i-2}-x_{i+1}} \right)$
$C_{i,2}^{r-1}$		$\frac{(x_i-x_{i-2})(x_i-x_{i-1})}{(x_{i+2}-x_{i-2})(x_{i+2}-x_{i-1})}$

for the term $f_{i-(r-1)+k}$ in Eq. (6) we get:

$$\begin{aligned} & \sum_{t=0}^k \frac{C_{i,t}^{r-1}}{x_{i-(r-1)+k} - x_i} \prod_{s \in \mathcal{I}_{i,t}^r \setminus \{i, i-(r-1)+k\}} \frac{x_i - x_s}{x_{i-(r-1)+k} - x_s} \\ &= \frac{1}{x_{i-(r-1)+k} - x_i} \prod_{s \in \mathcal{I}_{i,0}^{2r-1} \setminus \{i, i-(r-1)+k\}} \frac{x_i - x_s}{x_{i-(r-1)+k} - x_i}. \end{aligned}$$

Then,

$$\begin{aligned} C_{i,k}^{r-1} &= \prod_{s \in \mathcal{I}_{i,0}^{2r-1} \setminus \mathcal{I}_{i,k}^r} \frac{x_i - x_s}{x_{i-(r-1)+k} - x_s} - \sum_{t=0}^{k-1} C_{i,t}^{r-1} \prod_{s \in \mathcal{I}_{i,t}^r \setminus \mathcal{I}_{i,k}^r} \frac{x_i - x_s}{x_{i-(r-1)+k} - x_s} \\ & \quad \prod_{s \in \mathcal{I}_{i,k}^r \setminus \mathcal{I}_{i,t}^r} \frac{x_{i-(r-1)+k} - x_s}{x_i - x_s}. \end{aligned}$$

□

In Tables 1 and 2, we show the values $C_{i,k}^{r-1}, 0 \leq k \leq r - 1$ for $r = 2, 3$ and 4.

If we take a uniform grid, the following corollary is a direct consequence by Prop. 1.1. We denote as $C_{i,k}^{r-1} = C_k^{r-1}$ because this value does not depend on the position i .

Corollary 1.2 *Using a uniform grid, the optimal weights for the approximation of derivative values are given by:*

$$C_k^{r-1} = \binom{r-1}{k}^2 \binom{2r-2}{r-1}^{-1}, \quad k = 0, \dots, r-1. \tag{7}$$

Proof From $x_i = ih$, using the Lagrange basis, we have that

$$\begin{aligned} L_{j,k}^{r-1}(x) &= \prod_{\substack{s=i-(r-1)+k \\ s \neq i}}^{i+k} \frac{x - sh}{(j-s)h} \rightarrow p_k^{r-1}(x) = \sum_{j=i-(r-1)+k}^{i+k} f_j L_{j,k}^{r-1}(x) \rightarrow \\ \frac{d}{dx} p_k^{r-1}(x_i) &= \sum_{\substack{j=i-(r-1)+k \\ j \neq i}}^{i+k} \left(\frac{f_i}{(i-j)h} + \frac{f_j}{(j-i)h} \prod_{\substack{s=i-(r-1)+k \\ s \neq i, j}}^{i+k} \frac{i-s}{j-s} \right). \end{aligned}$$

Analogously,

$$\frac{d}{dx} p_0^{2r-2}(x_i) = \sum_{\substack{j=i-(r-1) \\ j \neq i}}^{i+(r-1)} \left(\frac{f_i}{(i-j)h} + \frac{f_j}{(j-i)h} \prod_{\substack{s=i-(r-1) \\ s \neq i, j}}^{i+(r-1)} \frac{i-s}{j-s} \right).$$

Table 2 Optimal weights for $r = 4$ and a non-uniform grid

$r = 4$	
$C_{i,0}^{r-1}$	$\frac{(x_i - x_{i+1})(x_i - x_{i+2})(x_i - x_{i+3})}{(x_{i+1} - x_{i-3})(x_{i-3} - x_{i+2})(x_{i+3} - x_{i-3})}$
$C_{i,1}^{r-1}$	$(x_i - x_{i+2})(x_i - x_{i+3})(x_i - x_{i-3}) \left(x_{i+1}(x_{i+2} + x_{i+3} - x_{i-2} - x_{i-3}) + x_{i+2}(x_{i+3} - x_{i-2} - x_{i-3}) - x_{i+3}x_{i-2} - x_{i-2}x_{i-3} + x_{i-2}^2 + x_{i-3}^2 \right)$
$C_{i,2}^{r-1}$	$(x_{i-3} - x_{i+1})(x_{i+2} - x_{i-2})(x_{i+2} - x_{i-3})(x_{i-2} - x_{i+3})(x_{i+3} - x_{i-3})$
$C_{i,3}^{r-1}$	$(x_i - x_{i+3})(x_i - x_{i-2})(x_i - x_{i-3}) \left(x_{i+2}^2 + x_{i+2}(x_{i+3} - x_{i-1} - x_{i-2} - x_{i-3}) + x_{i+3}^2 + x_{i-1}x_{i-2} + x_{i-1}x_{i-3} + x_{i-2}x_{i-3} \right)$
$C_{i,3}^{r-1}$	$(x_{i-2} - x_{i+2})(x_{i+2} - x_{i-3})(x_{i+3} - x_{i-1})(x_{i+3} - x_{i-2})(x_{i+3} - x_{i-3})$
$C_{i,3}^{r-1}$	$\frac{(x_i - x_{i-1})(x_i - x_{i-2})(x_i - x_{i-3})}{(x_{i+3} - x_{i-1})(x_{i+3} - x_{i-2})(x_{i+3} - x_{i-3})}$

By induction on k , if $k = 0$ and $\xi = s - i$, then

$$C_0^{r-1} \frac{f_{i-(r-1)}}{-(r-1)h} \prod_{s=i-(r-1)+1}^i \frac{i-s}{i-(r-1)-s} = \frac{f_{i-(r-1)}}{-(r-1)h} \prod_{s=i-(r-1)+1}^{i+(r-1)} \frac{i-s}{i-(r-1)-s} \rightarrow$$

$$C_0^{r-1} = \prod_{s=i+1}^{i+(r-1)} \frac{i-s}{i-(r-1)-s} = \prod_{s=i+1}^{i+(r-1)} \frac{s-i}{s-i+(r-1)} = \prod_{\xi=1}^{r-1} \frac{\xi}{\xi+(r-1)} = \binom{2r-2}{r-1}^{-1}.$$

We suppose the result for $k - 1$ and calculate C_k^{r-1} , with $0 \leq t < k \leq r - 1$. Thus, since

$$\begin{aligned} \mathcal{I}_{i,0}^{2r-1} \setminus \mathcal{I}_{i,k}^r &= \{i - (r - 1), i - (r - 1) + 1, \dots, i - (r - 1) + k - 1, \\ &\quad i + k + 1, \dots, i + (r - 1)\}, \\ \mathcal{I}_{i,k}^r \setminus \mathcal{I}_{i,t}^r &= \{i + t + 1, \dots, i + k\}, \\ \mathcal{I}_{i,t}^r \setminus \mathcal{I}_{i,k}^r &= \{i - (r - 1) + t, \dots, i - (r - 1) + k - 1\}, \end{aligned} \tag{8}$$

we obtain:

$$\begin{aligned} \prod_{s \in \mathcal{I}_{i,0}^{2r-1} \setminus \mathcal{I}_{i,k}^r} \frac{x_i - x_s}{x_{i-(r-1)+k} - x_s} &= \prod_{s=i-(r-1)}^{i-(r-1)+k-1} \frac{x_i - x_s}{x_{i-(r-1)+k} - x_s} \prod_{s=i+k+1}^{i+(r-1)} \frac{x_i - x_s}{x_{i-(r-1)+k} - x_s} \\ &= \prod_{l=0}^{k-1} \frac{(r-1)-l}{k-l} \prod_{l=k+1}^{r-1} \frac{l}{l+(r-1)-k} \\ &= \binom{r-1}{k} \binom{2(r-1)}{r-1}^{-1} \binom{2(r-1)}{k}, \\ \prod_{s \in \mathcal{I}_{i,k}^r \setminus \mathcal{I}_{i,t}^r} \frac{x_i - x_s}{x_{i-(r-1)+k} - x_s} &= \prod_{s=i+t+1}^{i+k} \frac{x_i - x_s}{x_{i-(r-1)+k} - x_s} = \prod_{l=t+1}^k \frac{l}{l+(r-1)-k} \\ &= \frac{k!((r-1)-(k-t))!}{(r-1)!t!}, \\ &= \frac{k!((r-1)-(k-t))!(k-t)!}{(r-1)!t!(k-t)!} = \binom{k}{t} \binom{r-1}{k-t}^{-1}, \\ \prod_{s \in \mathcal{I}_{i,t}^r \setminus \mathcal{I}_{i,k}^r} \frac{x_i - x_s}{x_{i-(r-1)+k} - x_s} &= \prod_{s=i-(r-1)+t}^{i-(r-1)+k-1} \frac{x_i - x_s}{x_{i-(r-1)+k} - x_s} = \prod_{l=t}^{k-1} \frac{(r-1)-l}{k-l} \\ &= \binom{r-1}{k} \binom{r-1}{t}^{-1} \binom{k}{t}. \end{aligned} \tag{9}$$

Then, since

$$\binom{2(r-1)}{k} - \sum_{t=0}^{k-1} \binom{r-1}{t} \binom{r-1}{k-t} = \binom{r-1}{k},$$

Table 3 Optimal weights $r = 2, 3, 4, 5$ for a uniform grid

	C_0^{r-1}	C_1^{r-1}	C_2^{r-1}	C_3^{r-1}	C_4^{r-1}
$r = 2$	1/2	1/2	–	–	–
$r = 3$	1/6	2/3	1/6	–	–
$r = 4$	1/20	9/20	9/20	1/20	–
$r = 5$	1/70	8/35	18/35	8/35	1/70

by induction hypothesis, (9) and Prop. 1.1, we have:

$$\begin{aligned}
 C_k^{r-1} &= \prod_{s \in \mathcal{I}_{i,0}^{2r-1} \setminus \mathcal{I}_k^r} \frac{x_i - x_s}{x_{i-(r-1)+k} - x_s} - \sum_{t=0}^{k-1} C_t^{r-1} \prod_{s \in \mathcal{I}_{i,t}^r \setminus \mathcal{I}_{i,k}^r} \frac{x_i - x_s}{x_{i-(r-1)+k} - x_s} \\
 &\quad \prod_{s \in \mathcal{I}_{i,k}^r \setminus \mathcal{I}_{i,t}^r} \frac{x_{i-(r-1)+k} - x_s}{x_i - x_s} \\
 &= \binom{r-1}{k} \binom{2(r-1)}{r-1}^{-1} \binom{2(r-1)}{k} - \sum_{t=0}^{k-1} \binom{r-1}{t} \binom{2r-2}{r-1}^{-1} \\
 &\quad \binom{r-1}{k} \binom{r-1}{t}^{-1} \binom{k}{t} \binom{k}{t}^{-1} \binom{r-1}{k-t} \\
 &= \binom{r-1}{k} \binom{2(r-1)}{r-1}^{-1} \left(\binom{2(r-1)}{k} - \sum_{t=0}^{k-1} \binom{r-1}{t} \binom{r-1}{k-t} \right) \\
 &= \binom{r-1}{k} \binom{2(r-1)}{r-1}^{-1}.
 \end{aligned}$$

□

In Table 3, some optimal weights are shown. For $r = 3$, they are the optimal weights shown in Levy et al. (1999).

With these linear weights, we can use the following expressions for the nonlinear weights:

$$\omega_{i,k}^{r-1} = \frac{\alpha_{i,k}^{r-1}}{\sum_{j=0}^{r-1} \alpha_{i,j}^{r-1}}, \quad \text{where } \alpha_{i,k}^{r-1} = \frac{C_{i,k}^{r-1}}{(\epsilon + I_{i,k}^{r-1})^\theta}, \quad k = 0, \dots, r-1, \quad (10)$$

with $\sum_{k=0}^{r-1} \omega_{i,k}^{r-1} = 1$. In Eq. (10), the parameter θ is an integer that assures maximum order of accuracy close to the discontinuities. In our case, we will take $\theta \geq r$ and introduce the parameter $\epsilon > 0$; to avoid divisions by zero, we will set it to $\epsilon = 10^{-16}$. The values $I_{i,k}^{r-1}$ are called *smoothness indicators* for $f(x)$ on each sub-stencil of $r - 1$ points. There exist several expressions for $I_{i,k}^{r-1}$. For example, the indicators designed in Jiang and Shu (1996) and Levy et al. (1999) are

$$\tilde{I}_{i,k}^{r-1} = \sum_{l=1}^{r-1} (x_{i+1/2} - x_{i-1/2})^{2l-1} \int_{x_{i-1/2}}^{x_{i+1/2}} \left(\frac{d^l}{dx^l} P_{i,k}^{r-1}(x) \right)^2 dx. \quad (11)$$

These indicators are suitable for the approximation of the conservation laws (1) with discontinuities in their solutions. The results obtained using them for approximating the derivative values are not satisfactory because they do not correctly detect kink discontinuities. For

approximating the derivative values, suitable for the approximation of the Hamilton–Jacobi equations (1), the measurement of the smoothness indicators should start from the second derivative (Jiang and Peng 2000; Amat and Ruiz 2017). In this work, we use the formula given in Amat and Ruiz (2017) adapted to non-uniform grids:

$$I_{i,k}^{r-1} = \sum_{l=2}^{r-1} (x_{i+1/2} - x_{i-1/2})^{2l-1} \int_{x_{i-1/2}}^{x_{i+1/2}} \left(\frac{d^l}{dx^l} p_{i,k}^{r-1}(x) \right)^2 dx. \tag{12}$$

Recently, a new WENO-2r algorithm has been introduced in Amat et al. (2020) and Amat et al. (2021). It consists of exploiting a recursive process to calculate the nonlinear weights with the aim of obtaining progressive order of accuracy of the approximation close to discontinuities. In this paper, we adapt these ideas to obtain a new progressive WENO interpolator to approximate the derivative values. The paper is divided into the following sections: in Sect. 2, we show the algorithm and construct the new method for $r = 3$ and for $r = 4$. In Sect. 3, we generalize the results for any r and give a general expression for nonlinear optimal weights. In Sect. 4, we present a strategy to compute efficiently the smoothness indicators and study the order of accuracy. Finally, some numerical experiments and some conclusions are presented.

2 New WENO with progressive adaptation to discontinuities: cases $r = 3$ and $r = 4$

The new algorithm designed by Amat et al. in Amat et al. (2020) consists of using the Aitken’s interpolation process Abramowitz and Stegun (2010) to calculate progressive linear weights. For simplicity, we present two examples and in the next section we show the generalization for any r .

2.1 New WENO for $r = 3$ with progressive adaptation to discontinuities in non-uniform grids

Let $p_{i,0}^4$ be the polynomial which interpolates $\{x_{i-2}, x_{i-1}, x_i, x_{i+1}, x_{i+2}\}$, then it can be divided into two polynomials $p_{i,0}^3$ interpolating in $\{x_{i-2}, x_{i-1}, x_i, x_{i+1}\}$ and $p_{i,1}^3$ in $\{x_{i-1}, x_i, x_{i+1}, x_{i+2}\}$. Therefore, by Aitken’s process, we have that

$$p_{i,0}^4(x) = C_{i,0,0}^3(x)p_{i,0}^3(x) + C_{i,0,1}^3(x)p_{i,1}^3(x) = \frac{x - x_{i+2}}{x_{i-2} - x_{i+2}}p_{i,0}^3(x) + \frac{x - x_{i-2}}{x_{i+2} - x_{i-2}}p_{i,1}^3(x),$$

then as $p_{i,0}^3$ and $p_{i,1}^3$ interpolate f at x_i , i.e. $p_{i,0}^3(x_i) = p_{i,1}^3(x_i) = f_i$, we have that:

$$\begin{aligned} \frac{dp_{i,0}^4}{dx}(x) &= \frac{dC_{i,0,0}^3}{dx}(x)p_{i,0}^3(x) + C_{i,0,1}^3(x)\frac{dp_{i,0}^3}{dx}(x) + \frac{dC_{i,0,1}^3}{dx}(x)p_{i,1}^3(x) + C_{i,0,1}^3(x)\frac{dp_{i,1}^3}{dx}(x) \\ &= \frac{1}{(x_{i+2} - x_{i-2})}(p_{i,1}^3(x) - p_{i,0}^3(x)) - \left(\frac{x - x_{i+2}}{x_{i+2} - x_{i-2}}\right)\frac{dp_{i,0}^3}{dx}(x) \\ &\quad + \left(\frac{x - x_{i-2}}{x_{i+2} - x_{i-2}}\right)\frac{dp_{i,1}^3}{dx}(x) \rightarrow \\ \frac{dp_{i,0}^4}{dx}(x_i) &= \left(\frac{x_{i+2} - x_i}{x_{i+2} - x_{i-2}}\right)\frac{dp_{i,0}^3}{dx}(x_i) + \left(\frac{x_i - x_{i-2}}{x_{i+2} - x_{i-2}}\right)\frac{dp_{i,1}^3}{dx}(x_i). \end{aligned}$$

Analogously,

$$\begin{aligned} \frac{dp_{i,0}^3}{dx}(x_i) &= \left(\frac{x_{i+1} - x_i}{x_{i+1} - x_{i-2}} \right) \frac{dp_{i,0}^2}{dx}(x_i) + \left(\frac{x_i - x_{i-2}}{x_{i+1} - x_{i-2}} \right) \frac{dp_{i,1}^2}{dx}(x_i), \\ \frac{dp_{i,1}^3}{dx}(x_i) &= \left(\frac{x_{i+2} - x_i}{x_{i+2} - x_{i-1}} \right) \frac{dp_{i,1}^2}{dx}(x_i) + \left(\frac{x_i - x_{i-1}}{x_{i+2} - x_{i-1}} \right) \frac{dp_{i,2}^2}{dx}(x_i). \end{aligned}$$

Then, it is clear that:

$$\begin{aligned} C_i^2 &= (C_{i,0}^2, C_{i,1}^2, C_{i,2}^2) = C_{i,0,0}^3(C_{i,0,0}^2, C_{i,0,1}^2, 0) + C_{i,0,1}^3(0, C_{i,1,1}^2, C_{i,1,2}^2) \\ &= \left(\frac{x_{i+2} - x_i}{x_{i+2} - x_{i-2}} \right) \left(\left(\frac{x_{i+1} - x_i}{x_{i+1} - x_{i-2}} \right), \left(\frac{x_i - x_{i-2}}{x_{i+1} - x_{i-2}} \right), 0 \right) \\ &\quad + \left(\frac{x_i - x_{i-2}}{x_{i+2} - x_{i-2}} \right) \left(0, \left(\frac{x_{i+2} - x_i}{x_{i+2} - x_{i-1}} \right), \left(\frac{x_i - x_{i-1}}{x_{i+2} - x_{i-1}} \right) \right); \end{aligned}$$

then, we define:

$$\tilde{C}_i^2 = (\tilde{C}_{i,0}^2, \tilde{C}_{i,1}^2, \tilde{C}_{i,2}^2) = \tilde{\omega}_{i,0,0}^3(C_{i,0,0}^2, C_{i,0,1}^2, 0) + \tilde{\omega}_{i,0,1}^3(0, C_{i,1,1}^2, C_{i,1,2}^2),$$

where

$$\tilde{\omega}_{i,0,0}^3 = \frac{\tilde{\alpha}_{i,0,0}^3}{\tilde{\alpha}_{i,0,0}^3 + \tilde{\alpha}_{i,0,1}^3}, \quad \tilde{\omega}_{i,0,1}^3 = \frac{\tilde{\alpha}_{i,0,1}^3}{\tilde{\alpha}_{i,0,0}^3 + \tilde{\alpha}_{i,0,1}^3}, \tag{13}$$

with

$$\tilde{\alpha}_{i,0,0}^3 = \frac{C_{i,0,0}^3}{(\epsilon + I_{i,0,0}^3)^\theta}, \quad \tilde{\alpha}_{i,0,1}^3 = \frac{C_{i,0,1}^3}{(\epsilon + I_{i,0,1}^3)^\theta}, \tag{14}$$

where the smoothness indicators $I_{i,0,k_1}^3, k_1 = 0, 1$ in (14) will be defined in Sect. 4 based on those introduced in Levy et al. (1999). Finally, we apply WENO with the new nonlinear weights, i.e. we calculate:

$$\begin{aligned} \tilde{P}'_i(x_i) &= \sum_{k=0}^2 \tilde{\omega}_{i,k}^2 \frac{dp_{i,k}^2}{dx}(x_i), \quad \text{with } \tilde{\omega}_{i,k}^2 = \frac{\tilde{\alpha}_{i,k}^2}{\sum_{j=0}^2 \tilde{\alpha}_{i,j}^2}, \quad \text{and} \\ \tilde{\alpha}_{i,k}^2 &= \frac{\tilde{C}_{i,k}^2}{(\epsilon + I_{i,k}^2)^\theta}, \quad k = 0, 1, 2, \end{aligned}$$

with $I_{i,k}^2, k = 0, 1, 2$, being the smoothness indicators introduced in Eq. (11).

Using the same reasoning, as a corollary, we obtain the formulas for new nonlinear weights in the uniform grid case. Thus, we have that

$$\begin{aligned} \frac{dp_0^4}{dx}(x) &= \frac{dC_{0,0}^3}{dx}(x)p_0^3(x) + C_{0,1}^3(x)\frac{dp_0^3}{dx}(x) + \frac{dC_{0,1}^3(x)}{dx}p_1^3(x) + C_{0,1}^3(x)\frac{dp_1^3}{dx}(x) \\ &= \frac{1}{4h}(p_1^3(x) - p_0^3(x)) - \left(\frac{x - (i+2)h - a}{4h} \right) \frac{dp_0^3}{dx}(x) \\ &\quad + \left(\frac{x - (i-2)h - a}{4h} \right) \frac{dp_1^3}{dx}(x) \rightarrow \\ \frac{dp_0^4}{dx}(x_i) &= \frac{1}{2} \frac{dp_0^3}{dx}(x_i) + \frac{1}{2} \frac{dp_1^3}{dx}(x_i), \\ \frac{dp_0^3}{dx}(x_i) &= \frac{1}{3} \frac{dp_0^2}{dx}(x_i) + \frac{2}{3} \frac{dp_1^2}{dx}(x_i), \quad \frac{dp_1^3}{dx}(x_i) = \frac{2}{3} \frac{dp_1^2}{dx}(x_i) + \frac{1}{3} \frac{dp_2^2}{dx}(x_i). \end{aligned}$$

In this case, we will write $C_{k_2, k_3}^{k_1}(x_i) = C_{k_2, k_3}^{k_1}$ for any k_1, k_2, k_3 . Thus, we get:

$$\begin{aligned} C^2 &= (C_0^2, C_1^2, C_2^2) = C_{0,0}^3(C_{0,0}^2, C_{0,1}^2, 0) + C_{0,1}^3(0, C_{1,1}^2, C_{1,2}^2) \\ &= \frac{1}{2} \left(\frac{1}{3}, \frac{2}{3}, 0 \right) + \frac{1}{2} \left(0, \frac{2}{3}, \frac{1}{3} \right) = \left(\frac{1}{6}, \frac{2}{3}, \frac{1}{6} \right). \end{aligned}$$

We can see that the linear optimal weights, in this case, are similar to the weights shown in Levy et al. (1999).

Finally, we repeat the same steps to obtain nonlinear weights.

2.2 New WENO with progressive adaptation to discontinuities for $r = 4$ in non-uniform grids

We start with the polynomial $p_{i,0}^6$, which interpolates $\{x_{i-3}, x_{i-2}, x_{i-1}, x_i, x_{i+1}, x_{i+2}, x_{i+3}\}$ and apply the same process, i.e. we express the derivative value of this polynomial at x_i as a combination of the derivative values of the polynomials $p_{i,0}^5$ and $p_{i,1}^5$ at x_i , which interpolate at the nodes $\{x_{i-3}, x_{i-2}, x_{i-1}, x_i, x_{i+1}, x_{i+2}\}$ and $\{x_{i-2}, x_{i-1}, x_i, x_{i+1}, x_{i+3}\}$, respectively; then, again, using Aitken’s algorithm, we obtain:

$$\begin{aligned} p_{i,0}^6(x) &= \left(\frac{x_{i+3} - x}{x_{i+3} - x_{i-3}} \right) p_{i,0}^5(x) + \left(\frac{x - x_{i-3}}{x_{i+3} - x_{i-3}} \right) p_{i,1}^5(x) \rightarrow \\ \frac{dp_{i,0}^6}{dx}(x) &= \left(\frac{1}{x_{i+3} - x_{i-3}} \right) (p_{i,1}^5(x) - p_{i,0}^5(x)) + \left(\frac{x_{i+3} - x}{x_{i+3} - x_{i-3}} \right) \frac{dp_{i,0}^5}{dx}(x) \\ &\quad + \left(\frac{x - x_{i-3}}{x_{i+3} - x_{i-3}} \right) \frac{dp_{i,1}^5}{dx}(x) \rightarrow \\ \frac{dp_{i,0}^6}{dx}(x_i) &= \left(\frac{1}{x_{i+3} - x_{i-3}} \right) (p_{i,1}^5(x_i) - p_{i,0}^5(x_i)) + \left(\frac{x_{i+3} - x_i}{x_{i+3} - x_{i-3}} \right) \frac{dp_{i,0}^5}{dx}(x_i) \\ &\quad + \left(\frac{x_i - x_{i-3}}{x_{i+3} - x_{i-3}} \right) \frac{dp_{i,1}^5}{dx}(x_i). \end{aligned}$$

From $p_{i,1}^5(x_i) = p_{i,0}^5(x_i) = f_i$, we have:

$$\frac{dp_{i,0}^6}{dx}(x_i) = \left(\frac{x_{i+3} - x_i}{x_{i+3} - x_{i-3}} \right) \frac{dp_{i,0}^5}{dx}(x_i) + \left(\frac{x_i - x_{i-3}}{x_{i+3} - x_{i-3}} \right) \frac{dp_{i,1}^5}{dx}(x_i).$$

Analogously, we represent $p_{i,0}^5$ as a combination of $p_{i,0}^4$ and $p_{i,1}^4$ as

$$p_{i,0}^5(x) = \left(\frac{x_{i+2} - x}{x_{i+2} - x_{i-3}} \right) p_{i,0}^4(x) + \left(\frac{x - x_{i-3}}{x_{i+2} - x_{i-3}} \right) p_{i,1}^4(x),$$

and repeating the same steps we get:

$$\frac{dp_{i,0}^5}{dx}(x_i) = \left(\frac{x_{i+2} - x_i}{x_{i+2} - x_{i-3}} \right) \frac{dp_{i,0}^4}{dx}(x_i) + \left(\frac{x_i - x_{i-3}}{x_{i+2} - x_{i-3}} \right) \frac{dp_{i,1}^4}{dx}(x_i).$$

We repeat this procedure again to obtain:

$$\begin{aligned} \frac{dp_{i,1}^5}{dx}(x_i) &= \left(\frac{x_{i+3} - x_i}{x_{i+3} - x_{i-2}}\right) \frac{dp_{i,1}^4}{dx}(x_i) + \left(\frac{x_i - x_{i-2}}{x_{i+3} - x_{i-2}}\right) \frac{dp_{i,2}^4}{dx}(x_i), \\ \frac{dp_{i,0}^4}{dx}(x_i) &= \left(\frac{x_{i+1} - x_i}{x_{i+1} - x_{i-3}}\right) \frac{dp_{i,0}^3}{dx}(x_i) + \left(\frac{x_i - x_{i-3}}{x_{i+1} - x_{i-3}}\right) \frac{dp_{i,1}^3}{dx}(x_i), \\ \frac{dp_{i,1}^4}{dx}(x_i) &= \left(\frac{x_{i+2} - x_i}{x_{i+2} - x_{i-2}}\right) \frac{dp_{i,1}^3}{dx}(x_i) + \left(\frac{x_i - x_{i-2}}{x_{i+2} - x_{i-2}}\right) \frac{dp_{i,2}^3}{dx}(x_i), \\ \frac{dp_{i,2}^4}{dx}(x_i) &= \left(\frac{x_{i+3} - x_i}{x_{i+3} - x_{i-1}}\right) \frac{dp_{i,2}^3}{dx}(x_i) + \left(\frac{x_i - x_{i-1}}{x_{i+3} - x_{i-1}}\right) \frac{dp_{i,3}^3}{dx}(x_i), \end{aligned}$$

then, the optimal progressive weights are:

$$\begin{aligned} C_i^3 &= C_{i,0,0}^5 (C_{i,0,0}^4 (C_{i,0,0}^3, C_{i,0,1}^3, 0, 0) + C_{i,0,1}^4 (0, C_{i,1,1}^3, C_{i,1,2}^3, 0)) \\ &+ C_{i,0,1}^5 (C_{i,1,1}^4 (0, C_{i,1,1}^3, C_{i,1,2}^3, 0) + C_{i,1,2}^4 (0, 0, C_{i,2,2}^3, C_{i,2,3}^3)) \\ &= \left(\frac{x_{i+3} - x_i}{x_{i+3} - x_{i-3}}\right) \left(\left(\frac{x_{i+2} - x_i}{x_{i+2} - x_{i-3}}\right) \left(\left(\frac{x_{i+1} - x_i}{x_{i+1} - x_{i-3}}\right), \left(\frac{x_i - x_{i-3}}{x_{i+1} - x_{i-3}}\right), 0, 0\right) + \right. \\ &+ \left.\left(\frac{x_i - x_{i-3}}{x_{i+2} - x_{i-3}}\right) \left(0, \left(\frac{x_{i+2} - x_i}{x_{i+2} - x_{i-2}}\right), \left(\frac{x_i - x_{i-2}}{x_{i+2} - x_{i-2}}\right), 0\right)\right) + \\ &+ \left(\frac{x_i - x_{i-3}}{x_{i+3} - x_{i-3}}\right) \left(\left(\frac{x_{i+3} - x_i}{x_{i+3} - x_{i-2}}\right) \left(0, \left(\frac{x_{i+2} - x_i}{x_{i+2} - x_{i-2}}\right), \left(\frac{x_i - x_{i-2}}{x_{i+2} - x_{i-2}}\right), 0\right) + \right. \\ &+ \left.\left(\frac{x_i - x_{i-2}}{x_{i+3} - x_{i-2}}\right) \left(0, 0, \left(\frac{x_{i+3} - x_i}{x_{i+3} - x_{i-1}}\right), \left(\frac{x_i - x_{i-1}}{x_{i+3} - x_{i-1}}\right)\right)\right). \end{aligned}$$

Thus, we can define

$$\begin{aligned} \tilde{C}_i^3 &= \tilde{\omega}_{i,0,0}^5 (\tilde{\omega}_{i,0,0}^4 (C_{i,0,0}^3, C_{i,0,1}^3, 0, 0) + \tilde{\omega}_{i,0,1}^4 (0, C_{i,1,1}^3, C_{i,1,2}^3, 0)) \\ &+ \tilde{\omega}_{i,0,1}^5 (\tilde{\omega}_{i,1,1}^4 (0, C_{i,1,1}^3, C_{i,1,2}^3, 0) + \tilde{\omega}_{i,1,2}^4 (0, 0, C_{i,2,2}^3, C_{i,2,3}^3)), \end{aligned}$$

where

$$\begin{aligned} \tilde{\omega}_{i,0,0}^5 &= \frac{\tilde{\alpha}_{i,0,0}^5}{\tilde{\alpha}_{i,0,0}^5 + \tilde{\alpha}_{i,0,1}^5}, \quad \tilde{\omega}_{i,0,1}^5 = \frac{\tilde{\alpha}_{i,0,1}^5}{\tilde{\alpha}_{i,0,0}^5 + \tilde{\alpha}_{i,0,1}^5}, \quad \tilde{\omega}_{i,0,0}^4 = \frac{\tilde{\alpha}_{i,0,0}^4}{\tilde{\alpha}_{i,0,0}^4 + \tilde{\alpha}_{i,0,1}^4}, \\ \tilde{\omega}_{i,0,1}^4 &= \frac{\tilde{\alpha}_{i,0,1}^4}{\tilde{\alpha}_{i,0,0}^4 + \tilde{\alpha}_{i,0,1}^4}, \quad \tilde{\omega}_{i,1,1}^4 = \frac{\tilde{\alpha}_{i,1,1}^4}{\tilde{\alpha}_{i,1,1}^4 + \tilde{\alpha}_{i,1,2}^4}, \quad \tilde{\omega}_{i,1,1}^4 = \frac{\tilde{\alpha}_{i,1,2}^4}{\tilde{\alpha}_{i,1,1}^4 + \tilde{\alpha}_{i,1,2}^4}, \end{aligned}$$

with

$$\tilde{\alpha}_{i,k,k_1}^l = \frac{C_{i,k,k_1}^l}{(\epsilon + I_{i,k,k_1}^l)^\theta},$$

and $l = 4, 5, k = 0, 1, k_1 = k, k + 1$; and with this vector, we apply the classical WENO algorithm.

As a corollary, if the grid is uniform we get:

$$\begin{aligned} \frac{dp_0^6}{dx}(x_i) &= \frac{1}{2} \frac{dp_0^5}{dx}(x_i) + \frac{1}{2} \frac{dp_1^5}{dx}(x_i), \quad \frac{dp_0^5}{dx}(x_i) = \frac{2}{5} \frac{dp_0^4}{dx}(x_i) + \frac{3}{5} \frac{dp_1^4}{dx}(x_i), \quad \frac{dp_1^5}{dx}(x_i) \\ &= \frac{3}{5} \frac{dp_1^4}{dx}(x_i) + \frac{2}{5} \frac{dp_2^4}{dx}(x_i), \end{aligned}$$

$$\begin{aligned} \frac{dp_0^4}{dx}(x_i) &= \frac{1}{4} \frac{dp_0^3}{dx}(x_i) + \frac{3}{4} \frac{dp_1^3}{dx}(x_i), & \frac{dp_1^4}{dx}(x_i) &= \frac{1}{2} \frac{dp_1^3}{dx}(x_i) + \frac{1}{2} \frac{dp_2^3}{dx}(x_i), & \frac{dp_2^4}{dx}(x_i) \\ &= \frac{3}{4} \frac{dp_2^3}{dx}(x_i) + \frac{1}{4} \frac{dp_3^3}{dx}(x_i). \end{aligned}$$

Thus, it is easy to check that

$$\begin{aligned} C^3 &= C_{0,0}^5 (C_{0,0}^4 (C_{0,0}^3, C_{0,1}^3, 0, 0) + C_{0,1}^4 (0, C_{1,1}^3, C_{1,2}^3, 0)) + C_{0,1}^5 (C_{1,1}^4 (0, C_{1,1}^3, C_{1,2}^3, 0) \\ &\quad + C_{1,2}^4 (0, 0, C_{2,2}^3, C_{2,3}^3)) \\ &= \frac{1}{2} \left(\frac{2}{5} \left(\frac{1}{4}, \frac{3}{4}, 0, 0 \right) + \frac{3}{5} \left(0, \frac{1}{2}, \frac{1}{2}, 0 \right) \right) + \frac{1}{2} \left(\frac{3}{5} \left(0, \frac{1}{2}, \frac{1}{2}, 0 \right) + \frac{2}{5} \left(0, 0, \frac{3}{4}, \frac{1}{4} \right) \right) \\ &= \left(\frac{1}{20}, \frac{9}{20}, \frac{9}{20}, \frac{1}{20} \right). \end{aligned}$$

Finally, we perform the same algorithm to obtain the nonlinear weights.

3 General new WENO algorithm for derivative values and general optimal weights

In this section, we will generalize the method for any r . To compute the linear weights for each “level” we can prove the following lemma following the same ideas as in Amat et al. (2020), i.e. using Aitken’s process as in Sects. 2.1 and 2.2.

Lemma 3.1 *Let $0 < r - 1 \leq l \leq 2r - 3$ and $0 \leq k \leq (2r - 3) - l$. If we denote as $C_{i,k,k}^l$ and $C_{i,k,k+1}^l$ the values which satisfy:*

$$\frac{dp_{i,k}^{l+1}}{dx}(x_i) = C_{i,k,k}^l \frac{dp_{i,k}^l(x_i)}{dx} + C_{i,k,k+1}^l \frac{dp_{i,k+1}^l(x_i)}{dx}, \tag{15}$$

then

$$C_{i,k,k}^l = \frac{x_{i-(r-1)+k+l+1} - x_i}{x_{i-(r-1)+k+l+1} - x_{i-(r-1)+k}}, \quad C_{i,k,k+1}^l = \frac{x_i - x_{i-(r-1)+k}}{x_{i-(r-1)+k+l+1} - x_{i-(r-1)+k}}. \tag{16}$$

Proof Let $r - 1 \leq l \leq 2r - 3$ and $0 \leq k \leq (2r - 3) - l$. To obtain the interpolators $p_{i,k}^{l+1}$, $p_{i,k}^l$ and $p_{i,k+1}^l$, the stencils used are $\{x_{i-(r-1)+k}, \dots, x_{i-(r-1)+k+l+1}\}$, $\{x_{i-(r-1)+k}, \dots, x_{i-(r-1)+k+l}\}$ and $\{x_{i-(r-1)+k+1}, \dots, x_{i-(r-1)+k+l+1}\}$, respectively. Then, using Aitken’s interpolation process (Abramowitz and Stegun 2010), we obtain:

$$\begin{aligned} p_{i,k}^{l+1}(x) &= \left(\frac{x_{i-(r-1)+k+l+1} - x}{x_{i-(r-1)+k+l+1} - x_{i-(r-1)+k}} \right) p_{i,k}^l(x) \\ &\quad - \left(\frac{x_{i-(r-1)+k} - x}{x_{i-(r-1)+k+l+1} - x_{i-(r-1)+k}} \right) p_{i,k+1}^l(x). \end{aligned}$$

If we differentiate the previous expression:

$$\begin{aligned} \frac{dp_{i,k}^{l+1}}{dx}(x) &= \frac{1}{x_{i-(r-1)+k+l+1} - x_{i-(r-1)+k}} (p_{i,k+1}^l(x) - p_{i,k}^l(x)) + \\ &\quad \left(\frac{x_{i-(r-1)+k+l+1} - x}{x_{i-(r-1)+k+l+1} - x_{i-(r-1)+k}} \right) \frac{dp_{i,k}^l}{dx}(x) \\ &\quad - \left(\frac{x_{i-(r-1)+k} - x}{x_{i-(r-1)+k+l+1} - x_{i-(r-1)+k}} \right) \frac{dp_{i,k+1}^l}{dx}(x), \end{aligned}$$

since $p_{i,k+1}^l(x_i) = p_{i,k}^l(x_i)$, we get:

$$\begin{aligned} \frac{dp_{i,k}^{l+1}}{dx}(x_i) &= \left(\frac{x_{i-(r-1)+k+l+1} - x_i}{x_{i-(r-1)+k+l+1} - x_{i-(r-1)+k}} \right) \frac{dp_{i,k}^l}{dx}(x_i) \\ &\quad + \left(\frac{x_i - x_{i-(r-1)+k}}{x_{i-(r-1)+k+l+1} - x_{i-(r-1)+k}} \right) \frac{dp_{i,k+1}^l}{dx}(x_i). \end{aligned}$$

□

It is trivial to check that for all i , we have:

$$C_{i,k,k}^l + C_{i,k,k+1}^l = 1, \quad 0 < r - 1 \leq l \leq 2r - 3 \text{ and } 0 \leq k \leq (2r - 3) - l.$$

As a corollary, we can calculate the optimal weights if the grid is uniform.

Corollary 3.2 *Let $0 < r - 1 \leq l \leq 2r - 3$ and $0 \leq k \leq (2r - 3) - l$, if the grid is uniform, i.e. there exists $h = 1/J$ such that $x_j = a + j \cdot h$, $0 \leq j \leq J$ and we denote as $C_{k,k}^l$ and $C_{k,k+1}^l$ the values which satisfy:*

$$\frac{dp_k^{l+1}}{dx}(x_i) = C_{k,k}^l \frac{dp_k^l}{dx}(x_i) + C_{k,k+1}^l \frac{dp_{k+1}^l}{dx}(x_i); \tag{17}$$

then

$$C_{k,k}^l = \frac{k - (r - 1) + (l + 1)}{l + 1}, \quad C_{k,k+1}^l = \frac{(r - 1) - k}{l + 1}. \tag{18}$$

Proof It is direct by Lemma 3.1 and $x_j = a + j \cdot h$, $0 \leq j \leq J$. □

We apply Eq. (15) for each level and get:

$$\begin{aligned} \frac{dp_{i,0}^{2r-2}}{dx}(x_i) &= \sum_{j_0=0}^1 C_{i,0,j_0}^{2r-3} \frac{dp_{i,j_0}^{2r-3}}{dx}(x_i) = \sum_{j_0=0}^1 C_{i,0,j_0}^{2r-3} \left(\sum_{j_1=j_0}^{j_0+1} C_{i,j_0,j_1}^{2r-4} \frac{dp_{i,j_1}^{2r-4}}{dx}(x_i) \right) = \dots \\ &= \sum_{j_0=0}^1 C_{i,0,j_0}^{2r-3} \left(\sum_{j_1=j_0}^{j_0+1} C_{i,j_0,j_1}^{2r-4} \left(\dots \left(\sum_{j_{r-3}=j_{r-4}}^{j_{r-4}+1} C_{i,j_{r-4},j_{r-3}}^{r-2} \right. \right. \right. \\ &\quad \left. \left. \left(\sum_{j_{r-2}=j_{r-3}}^{j_{r-3}+1} C_{i,j_{r-3},j_{r-2}}^{r-1} \frac{dp_{i,j_{r-2}}^{r-1}}{dx}(x_i) \right) \dots \right) \right). \end{aligned} \tag{19}$$

Thus, if we define the weights and the vector $\mathbf{C}_{i,k}^{r-1}$ with $0 \leq k \leq r - 2$ as

$$\begin{aligned} \mathbf{C}_{i,0}^{r-1} &= (C_{i,0,0}^{r-1}, C_{i,0,1}^{r-1}, 0, \dots, 0), \mathbf{C}_{i,1}^{r-1} = (0, C_{i,1,1}^{r-1}, C_{i,1,2}^{r-1}, 0, \dots, 0), \dots, \mathbf{C}_{i,r-2}^{r-1} \\ &= (0, \dots, 0, C_{i,r-2,r-2}^{r-1}, C_{i,r-2,r-1}^{r-1}), \end{aligned} \tag{20}$$

where $C_{i,k,k}^{r-1}, C_{i,k,k+1}^{r-1}$ are defined in Eq. (16), then we get that:

$$\begin{aligned} &\sum_{j_0=0}^1 C_{i,0,j_0}^{2r-3} \left(\sum_{j_1=j_0}^{j_0+1} C_{i,j_0,j_1}^{2r-4} \left(\dots \left(\sum_{j_{r-3}=j_{r-4}}^{j_{r-4}+1} C_{i,j_{r-4},j_{r-3}}^{r-2} \mathbf{C}_{i,j_{r-3}}^{r-1} \right) \dots \right) \right) \\ &= (C_{i,0}^{r-1}, C_{i,1}^{r-1}, \dots, C_{i,r-1}^{r-1}) = \mathbf{C}_i^{r-1}, \end{aligned} \tag{21}$$

with $C_{i,k}^{r-1}, 0 \leq k \leq r - 1$ the optimal weights obtained in Prop. 1.1, Tables 1 and 2 for $r = 2, 3$ and 4. It is analogous in the uniform grid case.

We have a tree scheme, where each branch produces a polynomial of a determined degree. Now, the idea is to use all the points which are not contaminated by a discontinuity. To follow this idea, we reduce this branch to $O(h^2)$ using nonlinear weights as follows:

We substitute in Eq. (21) the linear weights by nonlinear weights

$$\omega_{i,k,k_1}^l = \frac{\alpha_{i,k,k_1}^l}{\alpha_{i,k,k}^l + \alpha_{i,k,k+1}^l}, \quad \alpha_{i,k,k_1}^l = \frac{C_{i,k,k_1}^l}{(\epsilon + I_{i,k,k_1}^l)^\theta}, \quad k_1 = k, k + 1, \tag{22}$$

where θ, ϵ are the parameters above-mentioned and I_{i,k,k_1}^l are smoothness indicators defined at level $l = r, \dots, 2r - 3$. Therefore, the last ingredient of this scheme is to define the indicators to “remove” (to obtain $O(h^2)$) the non-suitable branch. We will use the strategy used in Amat et al. (2020) explained in detail in Sect. 4.

Finally, we define the new weights as:

$$\begin{aligned} \tilde{\mathbf{C}}_i^{r-1} &= (\tilde{C}_{i,0}^{r-1}, \tilde{C}_{i,1}^{r-1}, \dots, \tilde{C}_{i,r-2}^{r-1}, \tilde{C}_{i,r-1}^{r-1}) \\ &= \sum_{j_0=0}^1 \omega_{0,j_0}^{2r-3} \left(\sum_{j_1=j_0}^{j_0+1} \omega_{i,j_0,j_1}^{2r-4} \left(\dots \left(\sum_{j_{r-3}=j_{r-4}}^{j_{r-4}+1} \omega_{i,j_{r-4},j_{r-3}}^{r-2} \mathbf{C}_{i,j_{r-3}}^{r-1} \right) \dots \right) \right). \end{aligned} \tag{23}$$

Using $\tilde{\mathbf{C}}_i^{r-1}$, we apply classical WENO and calculate $\tilde{P}'_i(x_i) = \sum_{k=0}^{r-1} \tilde{\omega}_{i,k}^{r-1} \frac{dP_{i,k}^{r-1}}{dx}(x_i)$ with

$$\tilde{\omega}_{i,k}^{r-1} = \frac{\tilde{\alpha}_{i,k}^{r-1}}{\sum_{j=0}^{r-1} \tilde{\alpha}_{i,j}^{r-1}}, \quad \text{and} \quad \tilde{\alpha}_{i,k}^{r-1} = \frac{\tilde{C}_{i,k}^{r-1}}{(\epsilon + I_{i,k}^{r-1})^\theta}, \quad k = 0, \dots, r - 1. \tag{24}$$

4 Smoothness indicators and analysis of the accuracy

Let us start with the analysis of the smoothness indicators presented by Amat and Ruiz in Amat and Ruiz (2017), Eq. (12):

$$\begin{aligned} I_{i,k}^{r-1} &= \sum_{l=2}^{r-1} (x_{i+1/2} - x_{i-1/2})^{2l-1} \int_{x_{i-1/2}}^{x_{i+1/2}} \left(\frac{d^l}{dx^l} P_{i,k}^{r-1}(x) \right)^2 dx \\ &= \sum_{l=2}^{r-1} \left(\frac{h_i + h_{i-1}}{2} \right)^{2l-1} \int_{x_{i-1/2}}^{x_{i+1/2}} \left(\frac{d^l}{dx^l} P_{i,k}^{r-1}(x) \right)^2 dx, \end{aligned}$$

$k = 0, \dots, r - 1$, in non-uniform grids. We use the same ideas introduced in Aràndiga et al. (2010). First of all, at the smooth zones we obtain $I_{i,k}^{r-1} = O(h^4)$ using the following adapted result proved in Amat and Ruiz (2017).

Lemma 4.1 *Let $0 \leq k \leq r - 1$ and $p_{i,k}^{r-1}$ the interpolating polynomial of degree $r - 1 \geq 2$ of f that uses the nodes of the stencil $S_{i,k}^r$. Then, the smoothness indicator obtained through (11) satisfy*

$$I_k^{r-1} = \begin{cases} O(h^4), & \text{if } f \text{ is smooth in } S_{i,k}^r, \\ O(h^2), & \text{if } f \text{ has a corner discontinuity in } S_{i,k}^r, \\ O(1), & \text{if } f \text{ is discontinuous in } S_{i,k}^r, \end{cases}$$

with $h = \max\{h_j : j = 0, \dots, J - 1\}$.

We will prove the following auxiliary lemmas using the ideas presented in Aràndiga et al. (2010).

Lemma 4.2 *Let $0 \leq k, k_1 \leq r - 1$ and let $I_{i,n}^{r-1}$, $n = k, k_1$ be smoothness indicators of f on the stencil $S_{i,n}^r = \{x_{i-(r-1)+n}, \dots, x_{i+n}\}$. If $f \in C^r([x_{i+n-(r-1)}, x_{i+n}])$, then*

$$I_{i,k}^{r-1} - I_{i,k_1}^{r-1} = O(h^{r+3}).$$

Proof Let $p_{i,k}^{r-1}, p_{i,k_1}^{r-1}$ be the two interpolating polynomials of f of degree $r - 1 \geq 2$ at nodes in the stencil $S_{i,n}^r$ $n = k, k_1$. As $k \neq k_1$ and $0 \leq k, k_1 \leq r - 1$ then $f \in C^r([x_{i-1}, x_{i+1}])$, if $1 \leq l \leq r - 1$, $x \in [x_{i-1/2}, x_{i+1/2}] \subset [x_{i-1}, x_{i+1}]$, we have that $|(p_{i,n}^{r-1}(x) - f(x))^{(l)}| \leq O(h^{r-l})$, and

$$\begin{aligned} \left| (f^{(l)}(x))^2 - ((p_{i,n}^{r-1}(x))^{(l)})^2 \right| &= \left| (f^{(l)}(x) - (p_{i,n}^{r-1}(x))^{(l)}) (f^{(l)}(x) + (p_{i,n}^{r-1}(x))^{(l)}) \right| \\ &\leq O(h^{r-l})O(1) = O(h^{r-l}). \end{aligned} \tag{25}$$

Therefore, we get

$$\begin{aligned} &\left| I_{i,n}^{r-1} - \sum_{l=2}^{r-1} \left(\frac{h_i + h_{i-1}}{2} \right)^{2l-1} \int_{x_{i-1/2}}^{x_{i+1/2}} (f^{(l)}(x))^2 dx \right| \\ &= \left| \sum_{l=2}^{r-1} \left(\frac{h_i + h_{i-1}}{2} \right)^{2l-1} \int_{x_{i-1/2}}^{x_{i+1/2}} \left(((p_{i,n}^{r-1}(x))^{(l)})^2 - (f^{(l)}(x))^2 \right) dx \right| \\ &\leq \sum_{l=2}^{r-1} \left(\frac{h_i + h_{i-1}}{2} \right)^{2l-1} \int_{x_{i-1/2}}^{x_{i+1/2}} \left| ((p_{i,n}^{r-1}(x))^{(l)})^2 - (f^{(l)}(x))^2 \right| dx \\ &\leq \sum_{l=2}^{r-1} \left(\frac{h_i + h_{i-1}}{2} \right)^{2l} O(h^{r-l}) \\ &\leq O(h^{r+3}). \end{aligned} \tag{26}$$

Thus, we obtain:

$$\begin{aligned} \left| I_{i,k}^{r-1} - I_{i,k_1}^{r-1} \right| &\leq \left| I_{i,k}^{r-1} - \sum_{l=2}^{r-1} \left(\frac{h_i + h_{i-1}}{2} \right)^{2l-1} \int_{x_{i-1/2}}^{x_{i+1/2}} \left(f^{(l)}(x) \right)^2 dx \right| \\ &\quad + \left| I_{i,k_1}^{r-1} - \sum_{l=2}^{r-1} \left(\frac{h_i + h_{i-1}}{2} \right)^{2l-1} \int_{x_{i-1/2}}^{x_{i+1/2}} \left(f^{(l)}(x) \right)^2 dx \right| \quad (27) \\ &= O(h^{r+3}). \end{aligned}$$

□

Lemma 4.3 Let $0 \leq k, k_1 \leq r - 1, 1 \leq \theta$ and let $I_n^{r-1}, n = k, k_1$ be smoothness indicators of f on the stencil $S_{i,n}^r = \{x_{i-(r-1)+n}, \dots, x_{i+n}\}$, and p_{i,k_1}^{r-1} be the interpolating polynomial of f at nodes in the stencil $S_{k_1}^r$. If $f \in C^r([x_{i+n-(r-1)}, x_{i+n}])$ and $\epsilon = O(h^4)$ or $I_{i,k_1}^{r-1} = O(h^4)$, then:

$$\frac{I_{i,k}^{r-1} - I_{i,k_1}^{r-1}}{\epsilon - I_{i,k_1}^{r-1}} = O(h^{r-1}), \quad (28)$$

and

$$\frac{1}{(\epsilon - I_{i,k}^{r-1})^\theta} = \frac{1 + O(h^{r-1})}{(\epsilon - I_{i,k_1}^{r-1})^\theta}. \quad (29)$$

Proof The proof of Eq. (28) is direct by Lemmas 4.1 and 4.2. To prove Eq. (29), we use the following algebraic manipulation (see Aràndiga et al. (2010)):

$$\frac{1}{(\epsilon + I_{i,k}^{r-1})^\theta} = \frac{1}{(\epsilon + I_{i,k_1}^{r-1})^\theta} + \frac{1}{(\epsilon + I_{i,k_1}^{r-1})^\theta} \left(\frac{I_{i,k_1}^{r-1} - I_{i,k}^{r-1}}{\epsilon + I_{i,k}^{r-1}} \sum_{j=0}^{\theta-1} \left(\frac{\epsilon + I_{i,k_1}^{r-1}}{\epsilon + I_{i,k}^{r-1}} \right)^j \right).$$

□

Notice that if $I_{i,k_1}^{r-1} = O(h^m)$ with $m > 4$ and $0 < \epsilon < h^m$ is a fixed value, then Lemma 4.3 is not satisfied and the optimal order is not obtained. This is explained in detail in Aràndiga et al. (2010). In all our experiments, as we have mentioned in Section 1, we have set $\epsilon = 10^{-16}$. This way, the order of accuracy of the smoothness indicators will be $O(h^4)$ at the smooth parts of the data. In the rest of the paper, we always consider these conditions.

Proposition 4.4 Let $0 \leq k \leq r - 1, 1 \leq \theta$ and $\omega_{i,k}^{r-1}$ the nonlinear weights defined in Eq. (10), then

$$\begin{aligned} \omega_{i,k}^{r-1} &= O(1), \quad \text{if } f \text{ is smooth in } S_{i,k}^r, \\ \omega_{i,k}^{r-1} &= O(h^{2m\theta}), \quad \text{if } f \text{ is not smooth in } S_{i,k}^r, \end{aligned}$$

with $m = 2$ if the discontinuity is in the function and $m = 1$ if the discontinuity is in the first derivative.

Also, if f is smooth in $\{x_{i-(r-1)}, \dots, x_{i+(r-1)}\}$, then:

$$\omega_{i,k}^{r-1} = C_{i,k}^{r-1} + O(h^{r-1}),$$

with $C_{i,k}^{r-1}$ being the optimal weights defined in Eq. (1.1).

Proof Let $0 \leq k, n < r - 1$. If f is smooth in S_n^r , then using (10) and Lemma 4.1:

$$\alpha_{i,n}^{r-1} = \frac{C_{i,n}^{r-1}}{(\epsilon + I_{i,n}^{r-1})^\theta} = O(h^{-4\theta}) \rightarrow \sum_{l=0}^{r-1} \alpha_{i,l}^{r-1} = O(h^{-4\theta}),$$

then it is clear that, if f is smooth in $S_{i,k}^r$:

$$\omega_{i,k}^{r-1} = \frac{\alpha_{i,k}^{r-1}}{\sum_{l=0}^{r-1} \alpha_{i,l}^{r-1}} = O(1),$$

and if f is not smooth in $S_{i,k}^r$:

$$\omega_{i,k}^{r-1} = \frac{\alpha_{i,k}^{r-1}}{\sum_{l=0}^{r-1} \alpha_{i,l}^{r-1}} = O(h^{2m\theta}),$$

with $m = 2$ being the discontinuity in the function and $m = 1$ the discontinuity in the first derivative. Finally, if f is smooth in $\{x_{i-(r-1)}, \dots, x_{i+(r-1)}\}$, we fix a value $0 \leq k_1 \leq r - 1$, and using (29) in Lemma 4.3, we get for all $0 \leq k \leq r - 1$:

$$\alpha_{i,k}^{r-1} = \frac{C_{i,k}^{r-1}}{(\epsilon + I_{i,k}^{r-1})^\theta} = \frac{C_{i,k}^{r-1}(1 + O(h^{r-1}))}{(\epsilon + I_{i,k_1}^{r-1})^\theta} \rightarrow \sum_{l=0}^{r-1} \alpha_{i,l}^{r-1} = \frac{1 + O(h^{r-1})}{(\epsilon + I_{i,k_1}^{r-1})^\theta}.$$

Therefore,

$$\omega_{i,k}^{r-1} = \frac{\alpha_{i,k}^{r-1}}{\sum_{l=0}^{r-1} \alpha_{i,l}^{r-1}} = \frac{\frac{C_{i,k}^{r-1}(1+O(h^{r-1}))}{(\epsilon+I_{i,k_1}^{r-1})^\theta}}{\frac{1+O(h^{r-1})}{(\epsilon+I_{i,k_1}^{r-1})^\theta}} = \frac{C_{i,k}^{r-1}(1 + O(h^{r-1}))}{1 + O(h^{r-1})} = C_{i,k}^{r-1}(1 + O(h^{r-1})).$$

□

To construct the smoothness indicators for each “level”, we consider where the discontinuities are placed. To clarify the explanation, we start with an example, for $r = 4$. In Sect. 2.2, we have seen that we should define I_{i,k,k_1}^l with $l = 4, 5, k = 0, 1, k_1 = k, k + 1$, then we have the following scheme:

We suppose that the discontinuities are far enough from each other, i.e. there only exists one discontinuity at an interval. Thus, we have the following cases:

- There does not exist any discontinuity: we use all the weights.
- There exists a discontinuity at (x_{i+2}, x_{i+3}) : In this case, the points that are used to construct the interpolator are $\{x_{i-3}, \dots, x_{i+2}\}$. Therefore, we have to obtain $\omega_{0,0}^5 = O(1)$, $\omega_{0,1}^5 = O(h^2)$, $\omega_{0,0}^4 = O(1)$ and $\omega_{0,1}^4 = O(1)$ (the rest of the weights are not important because $\omega_{0,1}^5 = O(h^2)$). Notice that using the scheme in Fig. 2, we choose $I_{i,0,0}^6 = I_{i,0,0}^3$ and we get the desired result.
- There exists a discontinuity at (x_{i+1}, x_{i+2}) : the largest stencil not contaminated by the discontinuity is $\{x_{i-3}, \dots, x_{i+1}\}$. Therefore, we have to obtain $\omega_{0,1}^5 = O(h^2)$ and $\omega_{0,0}^5 = O(1)$, $\omega_{0,0}^4 = O(1)$ and $\omega_{0,1}^4 = O(1)$. In Fig. 3, we write in red the branch that is not used because a discontinuity is contained in the stencil; in green, the stencil that is used although it contains a discontinuity, and in blue the stencils which do not contain any discontinuity. Therefore, we define $I_{i,0,0}^6 = I_{i,0,0}^3$ and $I_{i,1,1}^5 = I_{i,1,1}^3$.

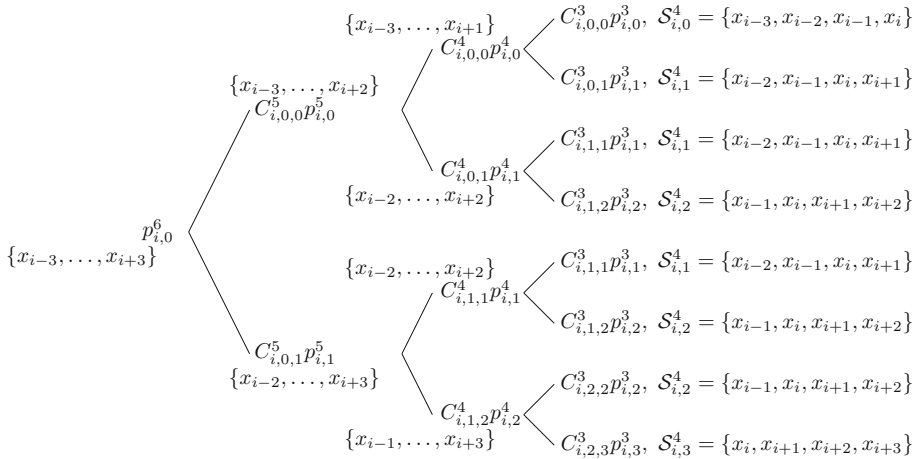


Fig. 1 Diagram showing the structure of the optimal weights needed to obtain optimal order of accuracy for $r = 4$

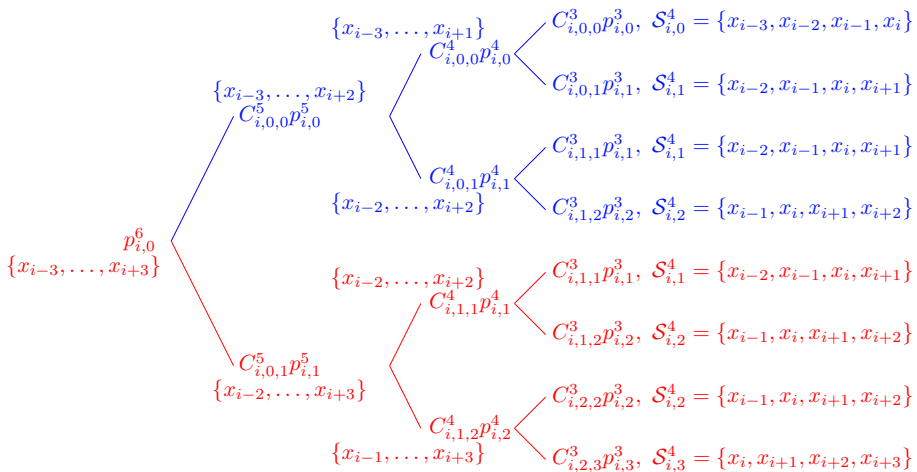


Fig. 2 First case: discontinuity at (x_i, x_{i+1}) . Red: polynomials that are not used. Blue: polynomials that are used

- There exists a discontinuity at (x_i, x_{i+1}) : the largest stencil that does not contain a discontinuity is $S_{i,0}^4 = \{x_{i-3}, \dots, x_i\}$. In this case, only the classical WENO interpolator can be recovered.
- The rest of the cases are symmetric.

Hence, if $I_{i,k}^{r-1}$, $k = 0, \dots, 3$ are the smoothness indicators defined in Eq. (11) for $r = 4$, then:

$$I_{i,0,0}^5 = I_{i,0}^3, I_{i,0,1}^5 = I_{i,3}^3, I_{i,0,0}^4 = I_{i,0}^3, I_{i,0,1}^4 = I_{i,2}^3, I_{i,1,1}^4 = I_{i,1}^3, I_{i,1,2}^4 = I_{i,3}^3. \quad (30)$$

Using this example, we introduce the following definition.

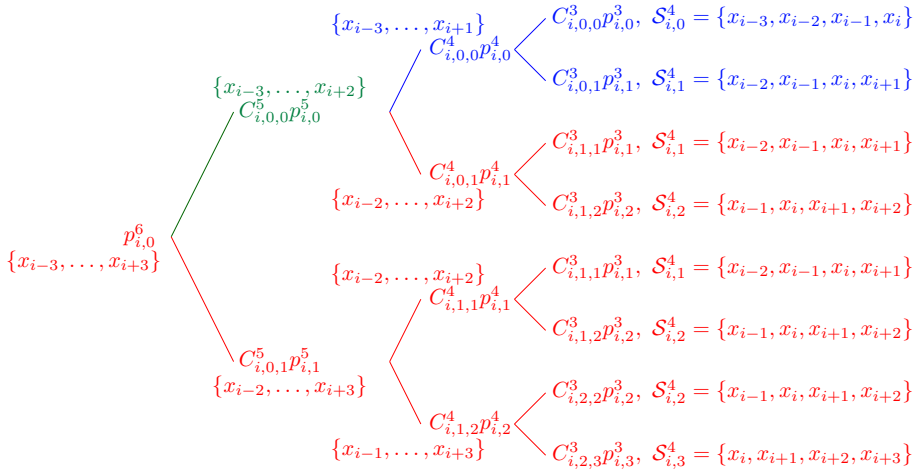


Fig. 3 Second case: discontinuity at (x_{i+1}, x_{i+2}) . Red: polynomials that are not used. Blue: polynomials used. Green: polynomial affected by a discontinuity, but not eliminated branch

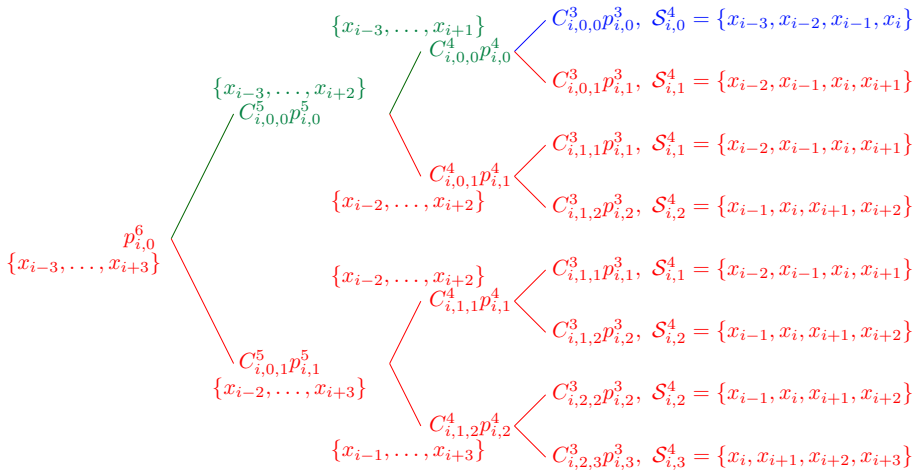


Fig. 4 Third case: discontinuity at (x_i, x_{i+1}) . Red: polynomials that are not used. Blue: polynomials used. Green: polynomial affected by a discontinuity but not eliminated branch

Definition 1 General smoothness indicators Let $I_{i,k}^{r-1}$, with $k = 0, \dots, r - 1$ be the smoothness indicators shown in Eq. (11), then we define the smoothness indicators for any r as:

$$\begin{aligned}
 I_{i,k,k}^l &= I_{i,k}^{r-1}, \quad k = 0, \dots, (2r - 3) - l, \\
 I_{i,k,k+1}^l &= I_{i,l+k+2-r}^{r-1}, \quad k = 0, \dots, (2r - 3) - l,
 \end{aligned}
 \tag{31}$$

with $r \leq l \leq 2r - 3$.

The following lemma is similar to Prop. 4.4 for nonlinear weights at each level.

Lemma 4.5 Let $r \leq l \leq 2r - 3$, $0 \leq k \leq (2r - 3) - l$, $1 \leq \theta$ and let w_{i,k,k_1}^l , with $k_1 = k, k + 1$ be the nonlinear weights defined in Eq. (22); then

1. If neither $I_{i,k,k}^l$ and $I_{i,k,k+1}^l$ are affected by a discontinuity, then $\omega_{i,k,k}^l = C_{i,k,k}^l(1 + O(h^{r-1}))$, $\omega_{i,k,k+1}^l = C_{i,k,k+1}^l(1 + O(h^{r-1}))$.
2. If $I_{i,k,k+1}^l$ is affected by a singularity, then $\omega_{i,k,k}^l = 1 + O(h^{2m\theta})$, $\omega_{i,k,k+1}^l = O(h^{2m\theta})$.
3. If $I_{i,k,k}^l$ is affected by a singularity, then $\omega_{i,k,k}^l = O(h^{2m\theta})$, $\omega_{i,k,k+1}^l = 1 + O(h^{2m\theta})$.

Here, $m = 2$ if the discontinuity is in the function, and $m = 1$ if the discontinuity is in the first derivative.

Proof It is similar to Prop. 4.4: from $C_{i,k,k}^l + C_{i,k,k+1}^l = 1$, using the definition given in (22), we have that:

1. If $I_{i,k,k}^l = O(h^4)$ and $I_{i,k,k+1}^l = O(h^4)$, by Eq. (29) in Lemma 4.3, we get:

$$\begin{aligned} \alpha_{i,k,k}^l &= \frac{C_{i,k,k}^l}{(\epsilon + I_{i,k,k}^l)^\theta} = \frac{C_{i,k,k}^l(1 + O(h^{r-1}))}{(\epsilon + I_{i,k,k+1}^l)^\theta}, \\ \omega_{i,k,k}^l &= \frac{\alpha_{i,k,k}^l}{\alpha_{i,k,k}^l + \alpha_{i,k,k+1}^l} = \frac{\frac{C_{i,k,k}^l(1 + O(h^{r-1}))}{(\epsilon + I_{i,k,k+1}^l)^\theta}}{\frac{C_{i,k,k}^l(1 + O(h^{r-1}))}{(\epsilon + I_{i,k,k+1}^l)^\theta} + \frac{C_{i,k,k+1}^l}{(\epsilon + I_{i,k,k+1}^l)^\theta}} \\ &= \frac{C_{i,k,k}^l(1 + O(h^{r-1}))}{C_{i,k,k}^l(1 + O(h^{r-1})) + C_{i,k,k+1}^l} \\ &= C_{i,k,k}^l(1 + O(h^{r-1})). \end{aligned}$$

Analogously for $\omega_{i,k,k+1}^l$.

2. If $I_{i,k,k}^l = O(h^4)$ and $I_{i,k,k+1}^l = O(1)$, if the discontinuity is in the function or $I_{i,k,k+1}^l = O(h^2)$ if the discontinuity is in the first derivative:

$$\begin{aligned} \omega_{i,k,k}^l &= \frac{C_{i,k,k}^l(\epsilon + I_{i,k,k+1}^l)^\theta}{C_{i,k,k}^l(\epsilon + I_{i,k,k+1}^l)^\theta + C_{i,k,k+1}^l(\epsilon + I_{i,k,k}^l)^\theta} \\ &= \frac{C_{i,k,k}^l(\epsilon + I_{i,k,k+1}^l)^\theta}{C_{i,k,k}^l(\epsilon + I_{i,k,k+1}^l)^\theta + O(h^{4\theta})} = \frac{C_{i,k,k}^l(\epsilon + I_{i,k,k+1}^l)^\theta}{C_{i,k,k}^l(\epsilon + I_{i,k,k+1}^l)^\theta} \frac{1}{1 + \frac{O(h^{4\theta})}{C_{i,k,k}^l(\epsilon + I_{i,k,k+1}^l)^\theta}} \\ &= 1 + O(h^{2m\theta}), \\ \omega_{i,k,k+1}^l &= \frac{C_{i,k,k+1}^l(\epsilon + I_{i,k,k}^l)^\theta}{C_{i,k,k}^l(\epsilon + I_{i,k,k+1}^l)^\theta + C_{i,k,k+1}^l(\epsilon + I_{i,k,k}^l)^\theta} = \frac{O(h^{4\theta})}{O(h^{\tilde{m}\theta}) + O(h^{4\theta})} \\ &= O(h^{(4-\tilde{m})\theta}), \quad \tilde{m} = 0, 2. \end{aligned}$$

(32)

3. Analogously, if $I_{i,k,k}^l = O(1)$ and $I_{i,k,k+1}^l = O(h^{2m})$.

□

If we analyse the examples presented, we can determine a rule for the weights and try to prove it. In the first case, Fig. 2, the discontinuity is in the interval $(x_{i+(l_0-1)}, x_{i+(l_0-1)}) = (x_{i+2}, x_{i+3})$, (i.e. $l_0 = 3$), and we can see that the branch marked in red is the one corresponding to $p_{i,1}^5$; thus, $\omega_{i,0,1}^l = \omega_{i,0,1}^{(r-2)+l_0} = \omega_{i,0,1}^5$ should be $O(h^2)$. In the second case, Fig. 3, the discontinuity is in the interval (x_{i+1}, x_{i+2}) , ($l_0 = 2$), and the red branches in those corresponding to $p_{i,1}^4$, then $\omega_{i,0,1}^{(r-2)+l_0} = \omega_{i,0,1}^4$ and $\omega_{i,0,1}^5$ should be $O(h^2)$. We prove that

the weights of the different branches which contain a discontinuity go to 0 as $h \rightarrow 0$, in the following lemma.

Lemma 4.6 *Let $2 \leq l_0 \leq r - 1$. If f is smooth in $[x_{i-(r-1)}, x_{i+(r-1)}] \setminus (x_{i+(l_0-1)}, x_{i+l_0})$, then for all $(r - 2) + l_0 \leq l \leq 2r - 3$ the nonlinear weights defined in Eq. (22) satisfy:*

$$\omega_{i,0,0}^l = 1 + O(h^{2m\theta}), \quad \omega_{i,0,1}^l = O(h^{2m\theta}),$$

with $m = 2$ if the discontinuity is in the function and $m = 1$ if the discontinuity is in the first derivative.

Proof Let $2 \leq l_0 \leq r - 1$ and $(r - 2) + l_0 \leq l \leq 2r - 3$. If the discontinuity is in $(x_{i+(l_0-1)}, x_{i+l_0})$, then $I_{i,0}^{r-1} = O(h^4)$, since $S_0^r = \{x_{i-(r-1)}, \dots, x_i\}$ and $l_0 \geq 1$. Subsequently, the stencil used to calculate $I_{i,l+2-r}^{r-1}$ is $S_{i+2-r}^r = \{x_{i-(r-1)+l+2-r}, \dots, x_{i+l+2-r}\}$, as $(r - 2) + l_0 \leq l \leq 2r - 3$ then $l_0 \leq l + 2 - r$; therefore, $I_{i,l+2-r}^{r-1} = O(1)$ if the discontinuity is in the function or $I_{i,l+2-r}^{r-1} = O(h^2)$ if the function contains a kink discontinuity. By Def. 1, we have that $I_{i,0,1}^l = I_{i,l+2-r}^{r-1} = O(h^{\tilde{m}})$, $\tilde{m} = 0, 2$. Using Lemma 4.5, we finish the proof. \square

Lemma 4.7 *Let $2 \leq l_0 \leq r - 1$. If f is smooth in $[x_{i-(r-1)}, x_{i+(r-1)}] \setminus (x_{i+(l_0-1)}, x_{i+l_0})$, then for all $r \leq l \leq l_0 + (r - 2) - 1$ the nonlinear weights defined in Eq. (22) satisfy:*

$$\omega_{i,k,k}^l = C_{i,k,k}^l + O(h^{r-1}), \quad \omega_{i,k,k+1}^l = C_{i,k,k+1}^l + O(h^{r-1}), \quad 0 \leq k \leq l_0 + (r - 2) - 1 - l, \tag{33}$$

with C_{i,k,k_1}^l being $k_1 = k, k + 1$ defined in Eq. (16).

Proof Let $2 \leq l_0 \leq r - 1$ and $r \leq l \leq l_0 + (r - 2) - 1$. We analyse the stencils used to calculate $I_{i,k,k}^l$ and $I_{i,k,k+1}^l$ with $0 \leq k \leq l_0 + (r - 2) - 1 - l$. First of all, we take into account two previous considerations:

From $r \leq l$, we get:

$$0 \leq k \leq l_0 + (r - 2) - 1 - l \leq l_0 + (r - 2) - 1 - r = l_0 - 3, \tag{34}$$

and from $k \leq l_0 + (r - 2) - 1 - l$:

$$l + k + 2 - r \leq l + l_0 + (r - 2) - 1 - l + 2 - r = l_0 - 1. \tag{35}$$

By Def. 1, we have that:

1. $I_{i,k,k}^l = I_{i,k}^{r-1}$, then the stencil used is $S_{i,k}^r = \{x_{i-(r-1)+k}, \dots, x_{i+k}\}$. Using (34), the stencil does not cross the discontinuity and $I_{i,k,k}^l = I_{i,k}^{r-1} = O(h^4)$.
2. $I_{i,k,k+1}^l = I_{i,l+k+2-r}^{r-1}$, then the stencil used is $S_{i,l+k+2-r}^r = \{x_{i-(r-1)+l+k+2-r}, \dots, x_{i+l+k+2-r}\}$. Using (34), analogously, $I_{i,k,k+1}^l = I_{i,l+k+2-r}^{r-1} = O(h^4)$.

By Lemma 4.5, we get the result. \square

With the ingredients presented in the previous sections, we can prove the following lemma. We suppose that the isolated discontinuity is to the right of the point x_i . By symmetry, the analysis for the left side would be similar.

Lemma 4.8 *Let $2 \leq l_0 \leq r - 1$. If f is smooth in $[x_{i-(r-1)}, x_{i+(r-1)}] \setminus (x_{i+(l_0-1)}, x_{i+l_0})$, then the nonlinear weights $\tilde{\omega}_{i,k}^{r-1}$, $k = 0, \dots, r - 1$ defined in Eq. (24) satisfy:*

$$(\tilde{\omega}_{i,0}^{r-1}, \tilde{\omega}_{i,1}^{r-1}, \dots, \tilde{\omega}_{i,r-1}^{r-1}) = (\hat{C}_{i,0}^{r-1} + O(h^{r-1}), \hat{C}_{i,1}^{r-1} + O(h^{r-1}), \dots, \hat{C}_{i,l_0-1}^{r-1} + O(h^{r-1}), O(h^{2m\theta}), \dots, O(h^{2m\theta})), \quad (36)$$

with $m = 2$ if the discontinuity is in the function and $m = 1$ if the discontinuity is in the first derivative, and

$$\frac{dp_{i,0}^{r+l_0-2}}{dx}(x_i) = \sum_{k=0}^{l_0-1} \hat{C}_{i,k}^{r-1} \frac{dp_{i,k}^{r-1}}{dx}(x_i).$$

Proof Applying Eq. (19) to the interpolatory polynomial $p_{i,0}^{r+l_0-2}$ and Lemmas 4.6 and 4.7, we obtain that:

$$(\omega_{i,0}^{r-1}, \omega_{i,1}^{r-1}, \dots, \omega_{i,r-1}^{r-1}) = (\hat{C}_{i,0}^{r-1} + O(h^{r-1}), \hat{C}_{i,1}^{r-1} + O(h^{r-1}), \dots, \hat{C}_{i,l_0-1}^{r-1} + O(h^{r-1}), O(h^{2m\theta}), \dots, O(h^{2m\theta})), \quad (37)$$

with $m = 2$ if the discontinuity is in the function and $m = 1$ if the discontinuity is in the first derivative, with

$$\frac{dp_{i,0}^{r+l_0-2}}{dx}(x_i) = \sum_{k=0}^{l_0-1} \hat{C}_{i,k}^{r-1} \frac{dp_{i,k}^{r-1}}{dx}(x_i).$$

As $\sum_{k=0}^{l_0-1} \hat{C}_{i,k}^{r-1} = 1$, we get the result. □

Using Lemma 4.8, it is easy to prove the main result. We obtain a progressive order of approximation for the derivative values close to the discontinuities.

Theorem 4.9 Let $1 \leq l_0 \leq r - 1$ and let $\tilde{\omega}_{i,k}^{r-1}$ be defined in Eq. (24) with $\theta \geq r - 1$. If f is smooth in $[x_{i-(r-1)}, x_{i+(r-1)}] \setminus \Omega$ and f has a discontinuity at Ω , then

$$\sum_{k=0}^{r-1} \tilde{\omega}_k^{r-1} \frac{dp_{i,k}^{r-1}}{dx}(x_i) - \frac{df}{dx}(x_i) = \begin{cases} O(h^{2r-2}), & \text{if } \Omega = \emptyset; \\ O(h^{(r-2)+l_0}), & \text{if } \Omega = (x_{i+(l_0-1)}, x_{i+l_0}). \end{cases} \quad (38)$$

Also, if $l_0 > r - 1$, then:

$$\sum_{k=0}^{r-1} \tilde{\omega}_k^{r-1} \frac{dp_{i,k}^{r-1}}{dx}(x_i) - \frac{df}{dx}(x_i) = O(h^{2r-2}). \quad (39)$$

Proof If f is smooth in the stencil $\{x_{i-(r-1)+k}, \dots, x_{i-(r-1)+k+l}\}$, then $\frac{df}{dx}(x_i) - \frac{dp_{i,k}^l}{dx}(x_i) = O(h^l)$. Let $2 \leq l_0 \leq r - 1$, then

$$\begin{aligned} & \sum_{k=0}^{r-1} \tilde{\omega}_{i,k}^{r-1} \frac{dp_{i,k}^{r-1}}{dx}(x_i) - \frac{df}{dx}(x_i) \\ &= \sum_{k=0}^{r-1} \tilde{\omega}_{i,k}^{r-1} \frac{dp_{i,k}^{r-1}(x_i)}{dx} - \frac{dp_{i,0}^{l_0+r-2}}{dx}(x_i) + \frac{dp_{i,0}^{l_0+r-2}}{dx}(x_i) - \frac{df}{dx}(x_i) \\ &= \sum_{k=0}^{r-1} (\tilde{\omega}_{i,k}^{r-1} - \hat{C}_{i,k}^{r-1}) \frac{dp_{i,k}^{r-1}}{dx}(x_i) + O(h^{r+l_0-2}) \end{aligned}$$

$$\begin{aligned}
 &= \sum_{k=0}^{l_0-1} (\tilde{\omega}_k^{r-1} - \hat{C}_{i,k}^{r-1}) \left(\frac{dp_{i,k}^{r-1}}{dx}(x_i) - \frac{df}{dx}(x_i) \right) \\
 &\quad + \sum_{k=l_0}^{r-1} \tilde{\omega}_{i,k}^{r-1} \left(\frac{dp_{i,k}^{r-1}}{dx}(x_i) - \frac{df}{dx}(x_i) \right) + O(h^{r+l_0-2}) \\
 &= O(h^{r-1+r-1}) + O(h^{2m\theta}) + O(h^{r+l_0-2}) = O(h^{r+l_0-2}).
 \end{aligned}$$

□

Therefore, we have proved that, when the isolated discontinuities affect the stencil, we get maximal order in a neighbourhood of the interval where it is located. In the next section, we show some experiments that confirm this theoretical result.

5 Numerical experiments and conclusions

In this section, we present some numerical experiments to verify the theoretical results shown in previous sections. We will use the following function:

$$f_\eta(x) = \begin{cases} x^{10} - x^9 + x^8 - 4x^7 + x^6 + x^5 + x^4 + x^3 + 5x^2 + 3x, & x < 0, \\ \eta - (x^{10} - 2x^9 + 3x^8 - 8x^7 - 2x^6 + x^5 - 2x^4 - 3x^3 - 5x^2 + 3x), & x \geq 0, \end{cases} \tag{40}$$

discretized in the interval $[-\frac{\pi}{6}, 1 - \frac{\pi}{6}]$ using $J_q = 2^q + 1$ uniform spaced points where $\eta = 0, 10$. In the first case, the function f_0 is continuous, but it presents a discontinuity in the first derivative, and in the second case, f_{10} has a jump discontinuity. We denote the interval where the discontinuity is contained as (x_{i-1}, x_i) and compute the error as

$$e_{l_0}^q = \left| \frac{d}{dx} f(x_{i+l_0}) - ap(x_{i+l_0}) \right|, \tag{41}$$

with ap being the approximation of the derivative values using the following methods:

- [lin-($2r - 2$)] Linear Lagrange method using a centred stencil of $2r - 1$ points.
- [WENO-($2r - 2$)] Nonlinear using the classical WENO algorithm explained in Sect. 1, Eq. (3).
- [p-WENO-($2r - 2$)] New progressive order WENO algorithm introduced in this work.

Finally, we compute the numerical order of accuracy using the formula:

$$o_{l_0}^q = \frac{e_{l_0}^q}{e_{l_0}^{q+1}}. \tag{42}$$

We start using a large stencil of five points, i.e. $r = 3$, and, using the linear method, we expect to obtain four consecutive points where the order is lost. Using classical WENO method, we will typically obtain order 3 at the points where the order is lost using the linear method. Using the new algorithm, we expect to obtain progressive order of accuracy $(r - 1, r, 2r - 2) = (2, 3, 4)$. We show the results for $r = 3$ in Tables 4, 5 and 6 for f_0 and Tables 10, 11 and 12 for f_{10} . For $r = 4$, we can see the results in Tables 7, 8 and 9 for the first experiment and Tables 13, 14 and 15 for the second one. It is clear that the new algorithm produces better approximation close to the discontinuity. We obtain the same results to the left of the discontinuity. Finally, it is important to remark that if the function is continuous, but presents a discontinuity in the first derivative, i.e. a kink, we cannot use the smoothness indicators introduced in Eq. (11).

Table 4 Grid refinement analysis for the linear Lagrange method for $r = 3$ algorithm for the function in (40) for f_0 , i.e. $\eta = 0$

q	e_1^q	o_1^q	e_2^q	o_2^q	e_3^q	o_3^q	e_4^q	o_4^q	e_5^q	o_5^q	e_6^q	o_6^q
5	$2.1434e + 00$	-	$3.7751e - 01$	-	$3.8405e - 06$	-	$2.9591e - 06$	-	$1.5404e - 06$	-	$3.9272e - 07$	-
6	$1.2862e + 00$	0.74	$2.5516e - 01$	0.57	$2.6340e - 07$	3.87	$2.5774e - 07$	3.52	$2.4316e - 07$	2.66	$2.1983e - 07$	0.84
7	$4.2774e - 01$	1.59	$1.0322e - 02$	4.63	$1.6297e - 08$	4.01	$1.6477e - 08$	3.97	$1.6513e - 08$	3.88	$1.6406e - 08$	3.74
8	$3.5549e - 01$	0.27	$2.0643e - 02$	-1.00	$9.8526e - 10$	4.05	$9.9893e - 10$	4.04	$1.0103e - 09$	4.03	$1.0194e - 09$	4.01
9	$2.1099e - 01$	0.75	$4.1287e - 02$	-1.00	$6.0034e - 11$	4.04	$6.0590e - 11$	4.04	$6.1111e - 11$	4.05	$6.1589e - 11$	4.05

Table 5 Grid refinement analysis for the classical WENO method for $r = 3$ algorithm for the function in (40) for f_0 , i.e. $\eta = 0$

q	e_1^q	o_1^q	e_2^q	o_2^q	e_3^q	o_3^q	e_4^q	o_4^q	e_5^q	o_5^q	e_6^q	o_6^q
5	$2.2231e-03$	-	$5.1191e-04$	-	$4.9491e-06$	-	$4.7419e-06$	-	$2.6510e-06$	-	$2.1599e-06$	-
6	$5.2818e-04$	2.07	$1.1285e-04$	2.18	$2.6489e-07$	4.22	$2.9352e-07$	4.01	$3.1452e-07$	3.08	$3.2063e-07$	2.75
7	$2.6023e-04$	1.02	$3.3248e-05$	1.76	$1.4689e-08$	4.17	$1.5617e-08$	4.23	$1.6576e-08$	4.25	$1.7520e-08$	4.19
8	$3.1408e-05$	3.05	$6.3688e-06$	2.38	$8.4033e-10$	4.13	$8.6444e-10$	4.18	$8.9040e-10$	4.22	$9.1788e-10$	4.25
9	$7.7296e-06$	2.02	$1.5575e-06$	2.03	$5.0505e-11$	4.06	$5.1136e-11$	4.08	$5.1804e-11$	4.10	$5.2511e-11$	4.13

Table 6 Grid refinement analysis for the new WENO method for $r = 3$ algorithm for the function in (40) for f_0 , i.e. $\eta = 0$

q	e_1^q	o_1^q	e_2^q	o_2^q	e_3^q	o_3^q	e_4^q	o_4^q	e_5^q	o_5^q	e_6^q	o_6^q
5	$2.2187e-03$	-	$6.5048e-05$	-	$1.0293e-05$	-	$1.8900e-05$	-	$3.2851e-05$	-	$5.3130e-05$	-
6	$5.2818e-04$	2.07	$6.3719e-06$	3.35	$3.4382e-07$	4.90	$4.7387e-07$	5.32	$6.5198e-07$	5.65	$8.9250e-07$	5.90
7	$1.9464e-04$	1.44	$7.3526e-07$	3.12	$1.5543e-08$	4.47	$1.8318e-08$	4.69	$2.1531e-08$	4.92	$2.5284e-08$	5.14
8	$3.1377e-05$	2.63	$7.9347e-08$	3.21	$7.4984e-10$	4.37	$8.1986e-10$	4.48	$8.9371e-10$	4.59	$9.7210e-10$	4.70
9	$7.7296e-06$	2.02	$9.4094e-09$	3.08	$4.0669e-11$	4.20	$4.2700e-11$	4.26	$4.4769e-11$	4.32	$4.6879e-11$	4.37

Table 7 Grid refinement analysis for the linear Lagrange method for $r = 4$ algorithm for the function in (40) for f_0 , i.e. $\eta = 0$

q	e_1^q	o_1^q	e_2^q	o_2^q	e_3^q	o_3^q	e_4^q	o_4^q	e_5^q	o_5^q	e_6^q	o_6^q
5	2.0944e + 00	-	5.0417e - 01	-	7.5502e - 02	-	1.1512e - 07	-	1.1023e - 07	-	1.0457e - 07	-
6	1.1883e + 00	0.82	3.0828e - 01	0.71	5.1031e - 02	0.57	1.9137e - 09	5.91	1.8731e - 09	5.88	1.8353e - 09	5.83
7	6.2362e - 01	0.93	8.3483e - 02	1.88	2.0643e - 03	4.63	3.0962e - 11	5.95	3.0591e - 11	5.94	3.0230e - 11	5.92
8	5.4724e - 01	0.19	6.6970e - 02	0.32	4.1287e - 03	-1.00	4.9560e - 13	5.97	4.9072e - 13	5.96	4.8894e - 13	5.95
9	3.9448e - 01	0.47	3.3941e - 02	0.98	8.2573e - 03	-1.00	7.1054e - 15	6.12	1.1990e - 14	5.35	7.5495e - 15	6.02

Table 8 Grid refinement analysis for the classical WENO method for $r = 4$ algorithm for the function in (40) for f_0 , i.e. $\eta = 0$

q	e_1^q	o_1^q	e_2^q	o_2^q	e_3^q	o_3^q	e_4^q	o_4^q	e_5^q	o_5^q	e_6^q	o_6^q
5	$2.2540e-04$	-	$4.3785e-05$	-	$1.1494e-05$	-	$2.3057e-08$	-	$6.2325e-08$	-	$1.1981e-07$	-
6	$2.5893e-05$	3.12	$5.1171e-06$	3.10	$1.3371e-06$	3.10	$6.0856e-11$	8.57	$3.7701e-11$	10.69	$1.0798e-10$	10.12
7	$4.4945e-04$	-4.12	$3.7303e-04$	-6.19	$8.4739e-05$	-5.99	$3.6913e-12$	4.04	$2.3932e-12$	3.98	$1.3776e-12$	6.29
8	$4.4035e-07$	10.00	$3.5802e-07$	10.03	$7.3336e-09$	13.50	$1.0836e-13$	5.09	$9.5923e-14$	4.64	$8.0380e-14$	4.10
9	$4.5085e-08$	3.29	$8.8880e-09$	5.33	$2.3887e-09$	1.62	$2.2204e-15$	5.61	$3.9968e-15$	4.58	$1.7764e-15$	5.50

Table 9 Grid refinement analysis for the new WENO method for $r = 4$ algorithm for the function in (40) for f_0 , i.e. $\eta = 0$

q	e_1^q	o_1^q	e_2^q	o_2^q	e_3^q	o_3^q	e_4^q	o_4^q	e_5^q	o_5^q	e_6^q	o_6^q
5	$2.2758e-04$	-	$8.2213e-06$	-	$8.3659e-07$	-	$1.4049e-07$	-	$2.0247e-08$	-	$1.5088e-07$	-
6	$2.6096e-05$	3.12	$4.5246e-07$	4.18	$2.5666e-08$	5.03	$3.1740e-09$	5.47	$3.1643e-09$	2.68	$2.9024e-09$	5.70
7	$2.9276e-06$	3.16	$2.8320e-08$	4.00	$7.4517e-10$	5.11	$4.3556e-11$	6.19	$4.6446e-11$	6.09	$4.8595e-11$	5.90
8	$3.7307e-07$	2.97	$1.5179e-09$	4.22	$2.5495e-11$	4.87	$5.6133e-13$	6.28	$5.9375e-13$	6.29	$6.2617e-13$	6.28
9	$4.5639e-08$	3.03	$9.1202e-11$	4.06	$8.1535e-13$	4.97	$7.5495e-15$	6.22	$6.2172e-15$	6.58	$8.8818e-15$	6.14

Table 10 Grid refinement analysis for the linear Lagrange method for $r = 3$ algorithm for the function in (40) for f_{10} , i.e. $\eta = 10$

q	e_1^q	σ_1^q	e_2^q	σ_2^q	e_3^q	σ_3^q	e_4^q	σ_4^q	e_5^q	σ_5^q	e_6^q	σ_6^q
5	$1.8881e + 02$	-	$2.7044e + 01$	-	$3.8405e - 06$	-	$2.9591e - 06$	-	$1.5404e - 06$	-	$3.9272e - 07$	-
6	$3.7462e + 02$	-0.99	$5.3588e + 01$	-0.99	$2.6340e - 07$	3.87	$2.5774e - 07$	3.52	$2.4316e - 07$	2.66	$2.1983e - 07$	0.84
7	$7.4624e + 02$	-0.99	$1.0668e + 02$	-0.99	$1.6297e - 08$	4.01	$1.6477e - 08$	3.97	$1.6513e - 08$	3.88	$1.6406e - 08$	3.74
8	$1.4930e + 03$	-1.00	$2.1335e + 02$	-1.00	$9.8526e - 10$	4.05	$9.9893e - 10$	4.04	$1.0103e - 09$	4.03	$1.0194e - 09$	4.01
9	$2.9865e + 03$	-1.00	$4.2671e + 02$	-1.00	$6.0034e - 11$	4.04	$6.0590e - 11$	4.04	$6.1111e - 11$	4.05	$6.1589e - 11$	4.05

Table 11 Grid refinement analysis for the classical WENO method for $r = 3$ algorithm for the function in (40) for f_{10} , i.e. $\eta = 10$

q	e_1^q	o_1^q	e_2^q	o_2^q	e_3^q	o_3^q	e_4^q	o_4^q	e_5^q	o_5^q	e_6^q	o_6^q
5	2.2187e-03	-	5.1191e-04	-	4.9491e-06	-	4.7419e-06	-	2.6510e-06	-	2.1599e-06	-
6	5.2818e-04	2.07	1.1285e-04	2.18	2.6489e-07	4.22	2.9352e-07	4.01	3.1452e-07	3.08	3.2063e-07	2.75
7	1.2891e-04	2.03	2.6612e-05	2.08	1.4689e-08	4.17	1.5617e-08	4.23	1.6576e-08	4.25	1.7520e-08	4.19
8	3.1347e-05	2.04	6.3658e-06	2.06	8.4033e-10	4.13	8.6444e-10	4.18	8.9040e-10	4.22	9.1788e-10	4.25
9	7.7296e-06	2.02	1.5575e-06	2.03	5.0505e-11	4.06	5.1136e-11	4.08	5.1804e-11	4.10	5.2511e-11	4.13

Table 12 Grid refinement analysis for the new WENO method for $r = 3$ algorithm for the function in (40) for f_{10} , i.e. $\eta = 10$

q	e_1^q	o_1^q	e_2^q	o_2^q	e_3^q	o_3^q	e_4^q	o_4^q	e_5^q	o_5^q	e_6^q	o_6^q
5	$2.2187e-03$	-	$6.5048e-05$	-	$1.0293e-05$	-	$1.8900e-05$	-	$3.2851e-05$	-	$5.3130e-05$	-
6	$5.2818e-04$	2.07	$6.3719e-06$	3.35	$3.4382e-07$	4.90	$4.7387e-07$	5.32	$6.5198e-07$	5.65	$8.9250e-07$	5.90
7	$1.2891e-04$	2.03	$7.0503e-07$	3.18	$1.5543e-08$	4.47	$1.8318e-08$	4.69	$2.1531e-08$	4.92	$2.5284e-08$	5.14
8	$3.1347e-05$	2.04	$7.9345e-08$	3.15	$7.4984e-10$	4.37	$8.1986e-10$	4.48	$8.9371e-10$	4.59	$9.7210e-10$	4.70
9	$7.7296e-06$	2.02	$9.4094e-09$	3.08	$4.0669e-11$	4.20	$4.2700e-11$	4.26	$4.4769e-11$	4.32	$4.6879e-11$	4.37

Table 13 Grid refinement analysis for the linear Lagrange method for $r = 4$ algorithm for the function in (40) for f_{10} , i.e. $\eta = 10$

q	e_1^q	σ_1^q	e_2^q	σ_2^q	e_3^q	σ_3^q	e_4^q	σ_4^q	e_5^q	σ_5^q	e_6^q	σ_6^q
5	$1.9943e + 02$	-	$4.3171e + 01$	-	$5.4088e + 00$	-	$1.1512e - 07$	-	$1.1023e - 07$	-	$1.0457e - 07$	-
6	$3.9585e + 02$	-0.99	$8.5642e + 01$	-0.99	$1.0718e + 01$	-0.99	$1.9137e - 09$	5.91	$1.8731e - 09$	5.88	$1.8353e - 09$	5.83
7	$7.8871e + 02$	-0.99	$1.7058e + 02$	-0.99	$2.1335e + 01$	-0.99	$3.0962e - 11$	5.95	$3.0591e - 11$	5.94	$3.0230e - 11$	5.92
8	$1.5781e + 03$	-1.00	$3.4127e + 02$	-1.00	$4.2671e + 01$	-1.00	$4.9560e - 13$	5.97	$4.9072e - 13$	5.96	$4.8894e - 13$	5.95
9	$3.1569e + 03$	-1.00	$6.8263e + 02$	-1.00	$8.5342e + 01$	-1.00	$7.1054e - 15$	6.12	$1.1990e - 14$	5.35	$7.5495e - 15$	6.02

Table 14 Grid refinement analysis for the classical WENO method for $r = 4$ algorithm for the function in (40) for f_{10} , i.e. $\eta = 10$

q	e_1^q	o_1^q	e_2^q	o_2^q	e_3^q	o_3^q	e_4^q	o_4^q	e_5^q	o_5^q	e_6^q	o_6^q
5	2.2758e-04	-	4.3853e-05	-	1.1496e-05	-	2.3057e-08	-	6.2325e-08	-	1.1981e-07	-
6	2.6096e-05	3.12	5.1258e-06	3.10	1.3372e-06	3.10	6.0856e-11	8.57	3.7701e-11	10.69	1.0798e-10	10.12
7	3.1154e-06	3.07	6.1776e-07	3.05	1.6158e-07	3.05	3.6913e-12	4.04	2.3932e-12	3.98	1.3776e-12	6.29
8	3.7307e-07	3.06	7.4306e-08	3.06	1.9486e-08	3.05	1.0836e-13	5.09	9.5923e-14	4.64	8.0380e-14	4.10
9	4.5639e-08	3.03	9.1095e-09	3.03	2.3928e-09	3.03	2.2204e-15	5.61	3.9968e-15	4.58	1.7764e-15	5.50

Table 15 Grid refinement analysis for the new WENO method for $r = 4$ algorithm for the function in (40) for f_{10} , i.e. $\eta = 10$

q	e_1^q	o_1^q	e_2^q	o_2^q	e_3^q	o_3^q	e_4^q	o_4^q	e_5^q	o_5^q	e_6^q	o_6^q
5	2.2758e-04	-	8.2213e-06	-	8.3659e-07	-	1.4049e-07	-	2.0247e-08	-	1.5088e-07	-
6	2.6096e-05	3.12	4.5246e-07	4.18	2.5666e-08	5.03	3.1740e-09	5.47	3.1643e-09	2.68	2.9024e-09	5.70
7	3.1154e-06	3.07	2.5939e-08	4.12	7.9466e-10	5.01	4.3556e-11	6.19	4.6446e-11	6.09	4.8595e-11	5.90
8	3.7307e-07	3.06	1.5179e-09	4.09	2.5496e-11	4.96	5.6133e-13	6.28	5.9375e-13	6.29	6.2617e-13	6.28
9	4.5639e-08	3.03	9.1202e-11	4.06	8.1535e-13	4.97	7.5495e-15	6.22	6.2172e-15	6.58	8.8818e-15	6.14

6 Conclusions

In this work, a new WENO algorithm with progressive order of accuracy close to discontinuities has been introduced. It allows to calculate approximations of derivative values of a function using regular or non-regular grids. It is based on the same ideas used in Amat et al. (2020) which consist in using Aitken process to calculate the nonlinear weights. The explicit formulas for the optimal weights have been showed and the order of accuracy in each interval has been proved. Finally, some experiments have been presented that confirm the theoretical results obtained.

Funding Open Access funding provided thanks to the CRUE-CSIC agreement with Springer Nature.

Open Access This article is licensed under a Creative Commons Attribution 4.0 International License, which permits use, sharing, adaptation, distribution and reproduction in any medium or format, as long as you give appropriate credit to the original author(s) and the source, provide a link to the Creative Commons licence, and indicate if changes were made. The images or other third party material in this article are included in the article's Creative Commons licence, unless indicated otherwise in a credit line to the material. If material is not included in the article's Creative Commons licence and your intended use is not permitted by statutory regulation or exceeds the permitted use, you will need to obtain permission directly from the copyright holder. To view a copy of this licence, visit <http://creativecommons.org/licenses/by/4.0/>.

References

- Abramowitz M, Stegun IA (2010) Handbook of mathematical functions with formulas, graphs, and mathematical tables. Cambridge University Press, Dover, New York
- Amat S, Ruiz J (2017) New WENO smoothness indicators computationally efficient in presence of corner discontinuities. *J Sci Comput* 71:1265–1237
- Amat S, Ruiz J, Shu CW, Yáñez DF (2020) A new WENO-2r algorithm with progressive order of accuracy close to discontinuities. *SIAM J Numer Anal* 58(6):3448–3474
- Amat S, Ruiz J, Shu CW, Yáñez DF (2021) Cell-average WENO with progressive order of accuracy close to discontinuities with applications to signal processing. *Appl Math Comput* 403:126131
- Aràndiga F, Baeza A, Belda AM, Mulet P (2011) Analysis of WENO schemes for full and Global accuracy. *SIAM J Numer Anal* 49(2):893–915
- Aràndiga F, Belda AM, Mulet P (2010) Point-value WENO multiresolution applications to stable image compression. *J Sci Comput* 43(2):158–182
- Jiang G, Peng D (2000) Weighted ENO schemes for Hamilton-Jacobi equations. *SIAM J Sci Comput* 21:2126–2143
- Jiang G, Shu C-W (1996) Efficient implementation of weighted ENO schemes. *J Comput Phys* 126(1):202–228
- Levy D, Puppo G, Russo G (1999) Central WENO schemes for hyperbolic systems of conservation laws. *Math Modell Numer Anal* 33(3):547–571
- Liu X-D, Osher S, Chan T (1994) Weighted essentially non-oscillatory schemes. *J Comput Phys* 115:200–212
- Shu C-W (1999) High order weighted essentially nonoscillatory schemes for convection dominated problems. *SIAM Rev* 51(1):82–126
- Yáñez DF (2010) Learning multiresolution: transformaciones multiescala derivadas de la teoría de aprendizaje y aplicaciones. PhD. Thesis, Valencia

Publisher's Note Springer Nature remains neutral with regard to jurisdictional claims in published maps and institutional affiliations.

Authors and Affiliations

Sergio Amat¹ · Juan Ruiz-Álvarez¹ · Chi-Wang Shu² · Dionisio F. Yáñez³ 

Sergio Amat
sergio.amat@upct.es

Juan Ruiz-Álvarez
juan.ruiz@upct.es

Chi-Wang Shu
chi-wang_shu@brown.edu

¹ Departamento de Matemática Aplicada y Estadística, Universidad Politécnica de Cartagena, Cartagena, Spain

² Division of Applied Mathematics, Brown University, Providence, RI, USA

³ Departamento de Matemáticas, Facultad de Matemáticas, Universidad de Valencia, Valencia, Spain